2.3 Evaluation of pretreatment and interim PET images

Pretreatment FDG-PET/CT was performed for 15 cases, and the maximum standardized uptake value (SUV) of the most FDG-avid lesion was measured. Interim FDG-PET scan was performed after 1 cycle of chemotherapy in 4 cases, after 2 cycles of chemotherapy in 10 cases, after 3 cycles of chemotherapy in 7 cases and after 4 cycles of chemotherapy in 3 cases. Image evaluation was performed by physicians with >5 years of experience in nuclear medicine. Diagnostic criteria for response evaluation followed International Harmonization Project criteria [12].

2.4 Statistical analysis

Data were expressed as mean ± SD. Mann-Whitney's U-test was used for evaluating differences in diagnostic performance between DLBCL and Burkitt lymphoma. Overall survival (OS) was defined as the interval from interim PET to death from any cause. Univariate analysis by proportional hazards (Cox) regression was used to assess the value of prognostic factors for predicting OS. Survival curves were calculated according to the methods of Kaplan and Meier [13], with differences between groups analyzed using the log-rank test. Values of $p<0.05$ were considered statistically significant.

Table 1. Patient characteristics

Characteristic	Total	DLBCL	Burkitt	UN
Patients	24	13	11	—
Male	23	13	10	—
Median age, y (range)	42.2 (25-66)	45.6 (27-66)	38.3 (25-61)	—
ECOG performance status 3-4	10	5	5	1
Stage III/IV	17/24	6/13	11/11	—
Extranodal sites	22	12	10	—
Bonemarrow involvement	9	0	9	3
CNS involvement	4	0	4	—
Median Soluble IL-2 level	1,649	1,239	2,184	1
Median LDH level	1,779	273	3,149	—
LDH level (<400 IU/L)	20	9	11	3
Median CD4 count (cells/mm^3)	204	149	259	2
17 - 100 cells/L	8	6	2	—
101 - 493 cells/L	14	5	9	—
Median HIV viral load (range)	789,060	231,060	1,347,060	2
cART naive	15	6	9	—
EBER positive in biopsy tissue sample	12	6	6	6
CD20 positive	22	12	10	—

DLBCL: diffuse large B cell lymphoma, UN: unknown, ECOG: Eastern Cooperative Oncology Group; LDH: lactate dehydrogenase, CNS: central nervous system, IL-2: interleukin-2 receptor, cART, combination antiretroviral therapy, EBER: Epstein-Barr virus-encoded small RNA.

3 Results

3.1 Patient characteristics

We retrospectively examined 24 HIV-infected patients (23 men, 1 woman; mean age, 42.2 years; range, 25-66 years). Patient characteristics are summarized in Table 1. After a median follow-up of 24 months (range, 2-57 months), 17 of 24 patients remained alive and 7 had died due to progression of ML. Patient characteristics are shown in Table 1. According to the malignancy criteria of the WHO, ML in the 24 HIV-infected patients was classified in DLBCL (n=13) or Burkitt lymphoma (n=11). Burkitt lymphoma in HIV-infected patients typically shows a more advanced stage at first diagnosis,

and a high incidence of bone marrow and CNS involvements. Mean CD4 counts, HIV viral load and Lactate Dehydrogenase (LDH) level were higher in Burkitt lymphoma than in DLBCL, however statistical significance was confirmed in LDH alone.

3.2 FDG-PET/CT images

Figures 1and 2 show the paradigm for FDG-PET/CT during the course of treatment for ML in HIV-infected patients (Figures 1 and 2). Pretreatment FDG-PET/CT was performed for 15 patients, comprising 12 patients for initial staging and 3 patients for restaging suspected ML recurrence. Interim FDG-PET/CT for the evaluation of therapeutic responses was performed in all 24 cases, and 10 cases were evaluated as "positive interim PET" and 14 cases were evaluated as "negative interim PET". Mean interval between pretreatment PET and interim PET was 56.4±21.9 days (range, 27-99 days).

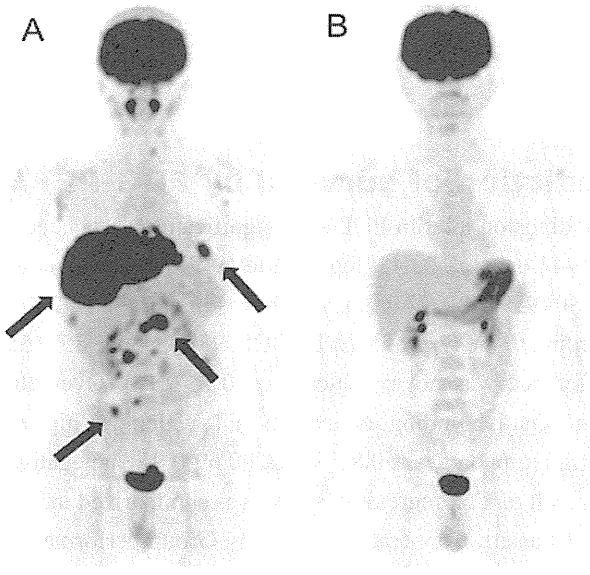

Figure 1. A. The pretreatment PET/CT shows multiple FDG avid lesions (arrows) for HIV related ML (DLBCL) and small focal FDG uptakes. B. Interim PET/CT shows disappearance of all FDG avid lesions. Long OS with 1,328 days was confirmed in this case.

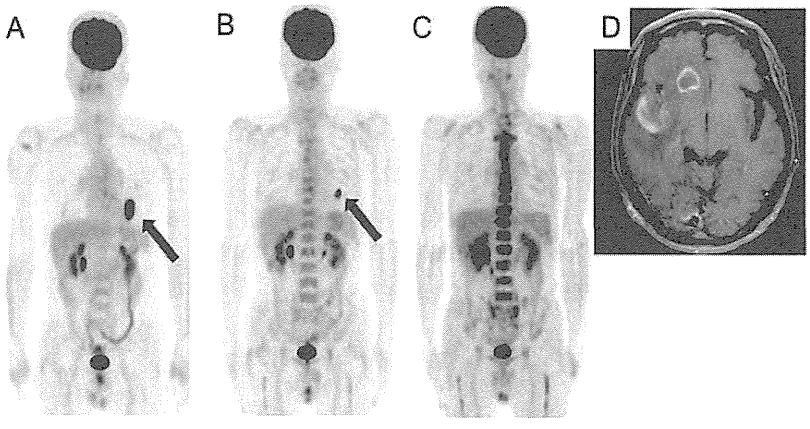

Figure 2. A. The pretreatment PET/CT shows FDG avid lesions at the left lung. B. Interim PET/CT shows residual FDG uptake at the lung. C. Follow-up PET/CT shows disappearance of the lesions but CNS ML was confirmed. This case showed short OS (134 days).

Mean SUVmax of FDG uptake by lymphoma lesions was 15.6±7.3 in ML patients on pretreatment FDG-PET/CT. No significant difference in FDG accumulation was seen between DLBCL (n=10, 15.7±8.0) and Burkitt lymphoma (n=5, 15.3±5.3).

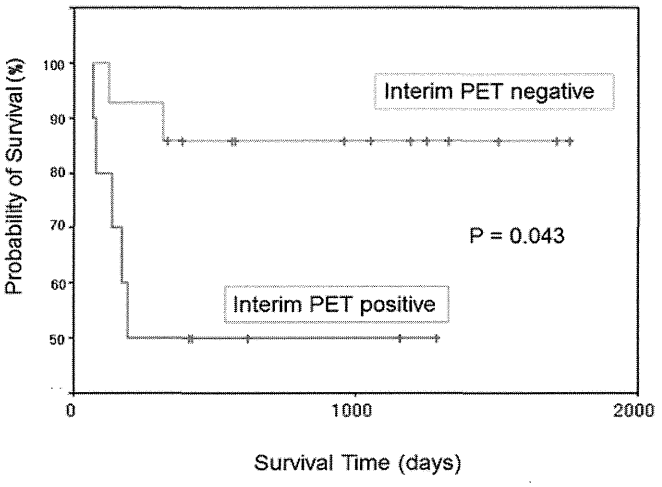

Figure 3. Kaplan-Meier Survival Estimates: Negative findings on interim PET showed longer OS compared with positive cases (p=0.043). Over all two year survival rate of negative findings on interim PET was 80%, which was higher than 29% in positive cases

3.3 Prediction of survival by FDG-PET/CT and other indices

Negative findings on interim PET were significantly associated with longer OS (932±549 days) compared with positive cases (454±442 days; p=0.043, log-rank test) (Figure 3). Over all two year survival rate of negative findings on interim PET was 0.80 (95%CI 0.69-0.91), which was higher than 0.29 (95%CI 0.16-0.41) in positive cases. A similar trend was found according to the type of ML (DLBCL, 934±593 vs. 557±556 days; Burkitt lymphoma, 931±550 vs. 229±136 days), but the difference was not significant (p=0.15-0.16). Over all two year survival rate in DLBCL was 0.80 (95%CI 0.69-0.91) in negative findings on interim PET, which was higher than 0.40 (95%CI 0.27-0.53). Over all two year survival rate in Burkitt lymphoma was 0.80 (95%CI 0.69-0.91) in negative findings on interim PET and no alive patient in positive cases. The result of Cox regression analysis is summarized in Table 2. Cox regression analysis showed strong prognostic influences of Eastern Cooperative Oncology Group performance status (ECOG-PS) (p=0.03) and interim PET findings (p=0.07) in OS.

Table 2. Univariate analysis of OS to pretreatment prognostic factors and interim PET/CT interpretation

Index	HR	95% CI for HR	P value
Age ≦40 vs. < 40	1.37	0.28 - 0.68	0.704
ECOG performance status 2-4 vs. 1	10.52	1.26 - 87.82	0.030
Stage III/IV vs. I/II	3.91	0.06 - 27.84	0.274
Bone marrow involvement	1.17	0.24 - 5.83	0.844
CNS involvement	2.21	0.43 - 11.52	0.346
Bulky mass	1.13	0.21 - 6.17	0.888
Soluble interleukin-2 receptor ≦1000 vs. < 1000	2.27	0.42 - 12.46	0.344
CD4 count, cells/L (cells/mm^3) ≦100 vs. < 100	0.47	0.10 - 2.36	0.362
HIV viral load	2.33	0.27 - 19.98	0.440
LDH level (< 400 IU/L)	0.47	0.09 - 2.58	0.385
cART naive	0.69	0.13 - 3.56	0.656
Pathology (DLBCL or Burkitt)	1.36	0.30 - 6.11	0.686
EBER positive in biopsy tissue sample	0.94	0.13 - 6.67	0.950
SUVmax of lesion in pretreatment PET ≦15 vs. < 15	1.64	0.10 - 26.35	0.726
Interim PET/CT positive vs. negative	4.57	0.88 - 23.73	0.070

OS: overall survival, HR: hazard ratio, ECOG: Eastern Cooperative Oncology Group, CNS:central nervous system, LDH: lactate dehydrogenase, cART:combination antiretroviral therapy, EBER: Epstein-Barr virus-encoded small RNA, DLBCL: diffuse large B cell lymphoma, SUV: standardized uptake value

4 Discussion

The present findings indicate that negative findings on interim FDG-PET/CT were strongly associated with improved OS in HIV-related ML. No other indices related to HIV or HIV-related ML (excluding ECOG-PS) showed a close relation to OS.

FDG-PET and PET/CT are well established for initial staging and restaging of ML, and have been adopted for determining therapeutic response in DLBCL [12, 14]. Although FDG-PET and PET/CT have demonstrated promising results for managing ML other than DLBCL, the role of FDG-PET/CT in other histologies (including HIV-related lymphoma) is not guaranteed [15].

DLBCL and Burkitt lymphoma account for the majority (90%) of ML cases [16], and these lymphomas are intensely FDG-avid [17, 18]. AIDS-related NHLs are characterized by high grade, aggressive nature and wide dissemination at the time of diagnosis, with the frequent involvement of extranodal sites [3]. Burkitt lymphoma is an aggressive disease requiring short-duration high-intensity chemotherapy regimens, and poor prognosis is strongly associated with a failure to achieve complete remission [18]. FDG-PET/CT can contribute to screening for viable disease that is considered reversible upon successful implementation of treatment [19].

In our study, 9 patients did not undergo PET in the pretreatment stage, but these cases must have had a high potential for FDG-avidity in the pretreatment lesion confirmed by CT, considering the characteristics of HIV-related ML. Moreover, DLBCL and Burkitt's lymphoma tended to progress rapidly, therefore it sometimes could not have time to perform baseline FDG-PET/CT scan before initiation of therapy. It appeared to be a limitation of our study and inducing FDG-PET/CT for assessment of treatment response in HIV-related ML.

A small case study of patients with AIDS-related lymphoma showed that FDG-PET/CT provided more accurate initial staging compared with conventional examinations, and was useful to monitor treatment response. PET/CT is regarded as a reliable method for managing lymphoma in HIV-infected patients [20, 21].

Although there is little evidence for the utility of FDG-PET/CT in HIV-related lymphoma, this modality is expected to offer a potent imaging technique for managing HIV-related lymphoma, as for ML in non-HIV patients [2].

Our result suggested that interim FDG-PET/CT reflected prognosis in terms of the OS rate for patients with HIV-related ML. On the other hand, baseline FDG uptake for DLBCL and Burkitt lymphoma showed no significant correlations with OS. From the perspective of pathological type analysis, interim PET predicted OS but showed no significant difference between types of ML. This might be attributable to the small number of study cases, so further study with a larger number of cases is needed. Prediction of OS using interim PET would allow reconsideration of the therapeutic strategy for each individual case in the early stages. According to our study results, HIV-related ML (which mainly comprises high-grade ML) might be expected to achieve complete response by existing therapeutic strategies. Early prognostic prediction using interim PET may contribute to improved outcomes of therapy. However, the incidence of therapeutic stumbling blocks such as infection is higher among HIV-infected patients than among other patients, regardless of the decreasing incidence of opportunistic infections thanks to HAART. Mortality in our study was caused by progression of lymphoma, so further studies with HIV-related ML cases in various situations are needed.

As for pretreatment indicators, poor ECOG-PS (PS 2-4) was associated with shorter OS. ECOG-PS has been an important parameter in prognostic models for aggressive lymphomas [22, 23], and is included in the International Prognostic Index for aggressive NHL as a significant risk factor. According to our results, extranodal site involvement and stage beyond III or IV showed relatively higher hazard rate than other factors but having no statistical significance. LDH levels were not considered a risk factor, and age seemed to be an inadaptable factor because HIV-related ML was caused by HIV infection, which is more common among young adults. In addition, extranodal involvement is frequently observed in HIV

related ML despite of the OS. As a result, ECOG-PS offers a prognostic index in the pretreatment state, but may be problematic given the subjective nature of evaluation.

This study did not examine relationships between PET findings and progression-free survival (PFS). Lymphadenopathy is a common symptom among HIV-infected individuals, as HIV is disseminated throughout lymphoid tissues after gaining entry to the human body. Trapping of HIV-positive effector cells in lymphoid tissues induces inflammation and lymphocytes are activated and switch to glycolysis, resulting in increased ^{18}F-FDG uptake into lymph nodes among HIV-infected individuals [24-26]. Differentiation of HIV-related lymphadenopathy from ML thus poses a diagnostic problem. Lymphadenopathy related to ML is generally larger and shows more intense FDG uptake than HIV-related lymphadenopathy [27] and the differentiation of common sites of lymphadenopathy between HIV-related lymphadenopathy and HIV-related ML may contribute to correct diagnosis [2]. However, no reliable cut-off values have yet been determined. Moreover, the difficulty in differential diagnosis compounds the problem of interim PET, which is intended to evaluate therapeutic response based on variations in FDG uptake into lesions and/or eruption of new lesions. As a result, making clear decisions for PFS appears very difficult in HIV-infected subjects (Figure 4).

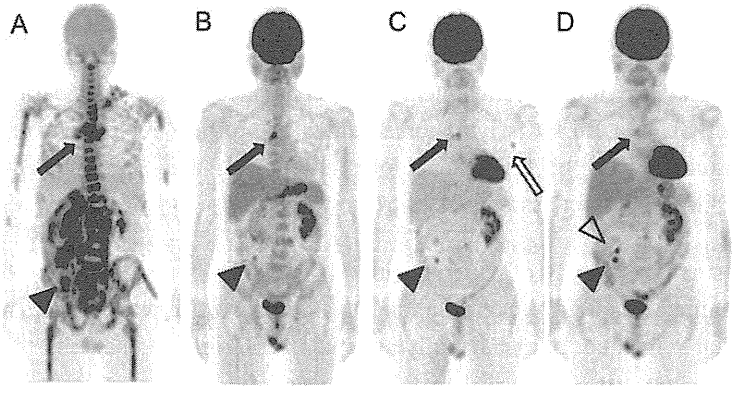

Figure 4. A. The pretreatment PET/CT shows FDG avid lesions at the mediastinum (arrow), cecum (arrow head). Interim (B) and follow up (C, D) PET/CT shows residual FDG uptake at both lesion. New FDG uptake appears at left axilla (C, white arrow) but disappeared (D), considered as HIV-related lymphadenopathy. New FDG uptake at cecum was caused by infection of tuberculosis (D white arrow head).

Key limitations in this study were the small sample size, variation of treatment regimens and 4 cases with evaluation of interim PET after only a single cycle of chemotherapy. Larger prospective studies with longer follow-up are needed to clarify our findings.

5 Conclusion

OS was longer for patients with HIV-related ML showing negative findings on interim FDG-PET than for patients with positive findings. Over all two year survival rate of negative findings on interim PET was higher than in positive cases. The strong prognostic influences for OS was ECOG-PS and interim PET findings. Interim FDG-PET can predict the prognosis of HIV-related ML. However, because of the limitations of the study, further prospective studies are needed in order to evaluate the value of FDG-PET/CT for HIV-related ML.

Acknowledgements

We thank Takashi Sato, Shingo Kawaguchi, Takuya Mitsumoto and Yoshiaki Taguchi for technical support. This work was supported by a Health and Labour Sciences Research Grant (HLSRG) from the Ministry of Health, Labour, and Welfare of Japan (Grant number: H22-AIDS-002). No other potential conflict of interest relevant to this article was reported.

Reference

[1] AIDS-Associated Viral Oncogenesis. 2007, pp: 69-127. Craig Meyers (Ed.). Springer Science+Business Media.

[2] Shiels MS, Pfeiffer RM, Gail MH, Hall HI, Li J, Chaturvedi AK et al. Cancer burden in the HIV-infected population in the United States. J Natl Cancer Inst. 2011; 103: 753-62. PMid:21483021 http://dx.doi.org/10.1093/jnci/djr076

[3] Patel P, Hanson DL, Sullivan PS, Novak RM, Moorman AC, Tong TC et al. Incidence of types of cancer among HIV-infected persons compared with the general population in the United States, 1992-2003. Ann Intern Med. 2008; 148: 728-36. PMid:18490686

[4] Grulich AE, van Leeuwen MT, Falster MO, Vajdic CM. Incidence of cancers in people with HIV/AIDS compared with immunosuppressed transplant recipients: a meta-analysis. Lancet. 2007; 370: 59-67. http://dx.doi.org/10.1016/S0140-6736(07)61050-2

[5] Mounier N, Spina M, Gisselbrecht C. Modern management of non-Hodgkin lymphoma in HIV-infected patients.Br J Haematol. 2007; 136: 685-98. PMid:17229246 http://dx.doi.org/10.1111/j.1365-2141.2006.06464.x

[6] Spano JP, Costagliola D, Katlama C, Mounier N, Oksenhendler E, Khayat D. AIDS-related malignancies: state of the art and therapeutic challenges. J Clin Oncol. 2008; 26: 4834-42. PMid:18591544 http://dx.doi.org/10.1200/JCO.2008.16.8252

[7] Jhanwar YS, Straus DJ. The role of PET in lymphoma. J Nucl Med. 2006; 47: 1326-34. PMid:16883013

[8] Sathekge M, Goethals I, Maes A, van de Wiele C. Positron emission tomography in patients suffering from HIV-1 infection. Eur J Nucl Med Mol Imaging. 2009; 36: 1176-84. PMid:19350235 http://dx.doi.org/10.1007/s00259-009-1126-9

[9] Sathekge M, Maes A, Kgomo M, et al. Van de Wiele C. Fluorodeoxyglucose uptake by lymph nodes of HIV patients is inversely related to CD4 cell count. Nucl Med Commun. 2010; 31: 137-40. PMid:19996812 http://dx.doi.org/10.1097/MNM.0b013e3283331114

[10] Liu Y. Demonstrations of AIDS-associated malignancies and infections at FDG PET-CT. Ann Nucl Med. 2011; 25: 536-46. PMid:21674240 http://dx.doi.org/10.1007/s12149-011-0506-y

[11] Dunleavy K, Wilson WH. How I treat HIV-associated lymphoma. Blood. 2012; 119: 3245-55. PMid:22337719 http://dx.doi.org/10.1182/blood-2011-08-373738

[12] Cheson BD, Pfistner B, Juweid ME, Gascoyne RD, Specht L, Horning SJ et al. Revised response criteria for malignant lymphoma. J Clin Oncol. 2007; 25: 579-86. PMid:17242396 http://dx.doi.org/10.1200/JCO.2006.09.2403

[13] Kaplan, E. L, Meier, P. Nonparametric estimation from incomplete observations. J. Amer. Statist. Assn. 1958; 53: 457-481. http://dx.doi.org/10.1080/01621459.1958.10501452

[14] Juweid ME, Stroobants S, Hoekstra OS, Mottaghy FM, Dietlein M, Guermazi A et al. Use of positron emission tomography for response assessment of lymphoma: consensus of the Imaging Subcommittee of International Harmonization Project in Lymphoma. J Clin Oncol. 2007; 25: 571-8. PMid:17242397 http://dx.doi.org/10.1200/JCO.2006.08.2305

[15] Jhanwar YS, Straus DJ. The role of PET in lymphoma. J Nucl Med. 2006; 47: 1326-1334. PMid:16883013

[16] Levine AM, Seneviratne L, Espina BM, Wohl AR, Tulpule A, Nathwani BN et al. Evolving characteristic of AIDS-related lymphoma. Blood. 2000; 96: 4084-90. PMid:11110677

[17] Tsukamoto N, Kojima M, Hasegawa M, Oriuchi N, Matsushima T, Yokohama A, et al. The usefulness of (18) F-fluorodeoxyglucose positron emission tomography ((18) F-FDG-PET) and a comparison of (18) F-FDG-pet with (67) gallium scintigraphy in the evaluation of lymphoma: relation to histologic subtypes based on the World Health Organization classification. Cancer. 2007; 110: 652-9. PMid:17582800 http://dx.doi.org/10.1002/cncr.22807

[18] Blum KA, Lozanski G, Byrd JC. Adult Burkitt leukemia and lymphoma. Blood. 2004; 104: 3009-3020. PMid:15265787 http://dx.doi.org/10.1182/blood-2004-02-0405

[19] Karantanis D, Durski JM, Lowe VJ, et al. 18F-FDG PET and PET/CT in Burkitt's lymphoma. Eur J Radiol. 2010; 75: e68-73. PMid:19716248 http://dx.doi.org/10.1016/j.ejrad.2009.07.035

[20] Just PA, Fieschi C, Baillet G, Galicier L, Oksenhendler E, Moretti JL et al. 18F-fluorodeoxyglucose positron tomography/computed tomography in AIDS-related Burkitt lymphoma. AIDS Patient Care STDS. 2008; 22: 695-700. PMid:18793085 http://dx.doi.org/10.1089/apc.2008.0174

[21] Goshen E, Davidson T, Avigdor A, Zwas TS, Levy I. PET/CT in the evaluation of lymphoma in patients with HIV-1 with suppressed viral loads. Clin Nucl Med. 2008; 33: 610-4. PMid:18716509 http://dx.doi.org/10.1097/RLU.0b013e3181813047

[22] Oken, M.M., Creech, R.H., Tormey, D.C, Horton J, Davis TE, McFadden ET, et al. Toxicity and Response Criteria of the Eastern Cooperative Oncology Group. Am J Clin Oncol. 1982; 5: 649-655. PMid:7165009 http://dx.doi.org/10.1097/00000421-198212000-00014

[23] A predictive model for aggressive non-Hodgkin's lymphoma. The International Non-Hodgkin's Lymphoma Prognostic Factors Project. N Engl J Med. 1993; 329: 987-94. PMid:8141877 http://dx.doi.org/10.1056/NEJM199309303291402

[24] Bakheet SM, Powe J. Benign causes of 18-FDG uptake on whole body imaging. Semin Nucl Med. 1998; 28: 352-358. http://dx.doi.org/10.1016/S0001-2998(98)80038-X

[25] Sugawara Y, Braun DK, Kison PV, Russo JE, Zasadny KR, Wahl RL. Rapid detection of human infections with fluorine-18 fluorodeoxyglucose and positron emission tomography: preliminary results. Eur J Nucl Med. 1998; 25: 1238-1243. PMid:9724371 http://dx.doi.org/10.1007/s002590050290

[26] Davison JM, Subramaniam RM, Surasi DS, Cooley T, Mercier G, Peller PJ. FDG PET/CT in patients with HIV. AJR Am J Roentgenol. 2011; 197: 284-94. PMid:21785073 http://dx.doi.org/10.2214/AJR.10.6332

[27] Castaigne C, Tondeur M, de Wit S, Hildebrand M, Clumeck N, Dusart M. Clinical value of FDGPET/CT for the diagnosis of human immunodeficiency virus-associated fever of unknown origin: a retrospective study. Nucl Med Commun. 2009; 30: 41-47. PMid:19306513 http://dx.doi.org/10.1097/MNM.0b013e328310b38d

JVI Journals.ASM.org

Distinct HIV-1 Escape Patterns Selected by Cytotoxic T Cells with Identical Epitope Specificity

Yuichi Yagita,[a] Nozomi Kuse,[a] Kimiko Kuroki,[b] Hiroyuki Gatanaga,[a,c] Jonathan M. Carlson,[d] Takayuki Chikata,[a] Zabrina L. Brumme,[e,f] Hayato Murakoshi,[a] Tomohiro Akahoshi,[a] Nico Pfeifer,[d] Simon Mallal,[g] Mina John,[g] Toyoyuki Ose,[b] Haruki Matsubara,[b] Ryo Kanda,[b] Yuko Fukunaga,[b] Kazutaka Honda,[a] Yuka Kawashima,[a] Yasuo Ariumi,[a] Shinichi Oka,[a,c] Katsumi Maenaka,[b] Masafumi Takiguchi[a]

Center for AIDS Research, Kumamoto University, Chuo-ku, Kumamoto, Japan[a]; Laboratory of Biomolecular Science, Faculty of Pharmaceutical Sciences, Hokkaido University, Kita-ku, Sapporo, Japan[b]; AIDS Clinical Center, National Center for Global Health and Medicine, Shinjuku-ku, Tokyo, Japan[c]; eScience Group, Microsoft Research, Los Angeles, California[d]; Faculty of Health Sciences, Simon Fraser University, Burnaby BC, Canada[e]; British Columbia Centre for Excellence in HIV/AIDS, Vancouver, BC, Canada[f]; Institute for Immunology & Infectious Diseases, Murdoch University, Murdoch, Western Australia, Australia[g]

Pol283-8-specific, HLA-B*51:01-restricted, cytotoxic T cells (CTLs) play a critical role in the long-term control of HIV-1 infection. However, these CTLs select for the reverse transcriptase (RT) I135X escape mutation, which may be accumulating in circulating HIV-1 sequences. We investigated the selection of the I135X mutation by CTLs specific for the same epitope but restricted by HLA-B*52:01. We found that Pol283-8-specific, HLA-B*52:01-restricted CTLs were elicited predominantly in chronically HIV-1-infected individuals. These CTLs had a strong ability to suppress the replication of wild-type HIV-1, though this ability was weaker than that of HLA-B*51:01-restricted CTLs. The crystal structure of the HLA-B*52:01-Pol283-8 peptide complex provided clear evidence that HLA-B*52:01 presents the peptide similarly to HLA-B*51:01, ensuring the cross-presentation of this epitope by both alleles. Population level analyses revealed a strong association of HLA-B*51:01 with the I135T mutant and a relatively weaker association of HLA-B*52:01 with several I135X mutants in both Japanese and predominantly Caucasian cohorts. An *in vitro* viral suppression assay revealed that the HLA-B*52:01-restricted CTLs failed to suppress the replication of the I135X mutant viruses, indicating the selection of these mutants by the CTLs. These results suggest that the different pattern of I135X mutant selection may have resulted from the difference between these two CTLs in the ability to suppress HIV-1 replication.

HIV-1-specific cytotoxic T cells (CTLs) play an important role in the control of HIV-1 replication (1–8); however, they also select immune escape mutations (9, 10). Population level adaptation of HIV to human leukocyte antigen (HLA) has been demonstrated (11–15), suggesting that HIV-1 can successfully adapt to immune responses previously effective against it.

It is well known that particular mutations can be selected by CTLs specific for a single HIV-1 epitope. On the other hand, studies on HLA-associated HIV-1 polymorphisms have revealed examples of particular mutations associated with multiple HLA class I alleles (16–21), suggesting that the same mutation can be selected by CTLs carrying different specificities in some cases. However, the selection of the same mutation by CTLs specific for different HIV-1 epitopes has rarely been reported. The change from Ala to Pro at residue 146 of Gag (A146P) is a well-analyzed case. A146P is an escape selected by not only HLA-B*57-restricted, ISW9-specific CTLs (22) but also by HLA-B*15:10-restricted and HLA-B*48:01-restricted CTLs (15, 23, 24), although the latter CTLs selected it by different mechanisms. The replacement of Thr with Asn at residue 242 (T242N) of Gag is another case. This mutant is selected by HLA-B*58:01-restricted and HLA-B*57-restricted CTLs specific for the TW10 epitope in HIV-1 clade B- and C-infected individuals (25–27).

The presence of Pol283-8(TAFTIPSI: TI8)-specific, HLA-B*51:01-restricted CTLs is associated with low viral loads in HIV-1-infected Japanese hemophiliacs, supporting an important role in the long-term control of HIV-1 infection (28). We previously showed that the frequency of a mutation at position 135 (I135X) of reverse transcriptase (RT) is strongly correlated with the prevalence of HLA-B*51 among nine cohorts worldwide and that this mutation is selected by Pol283-8(TAFTIPSI: TI8)-specific, HLA-B*51:01-restricted CTLs (15). Of these cohorts, a Japanese one showed the highest frequency of the I135X mutation in HLA-B*51:01 negatives (66% in a Japanese cohort and 11 to 29% in other cohorts). This finding may be explained by the fact that the Japanese cohort has the highest prevalence of HLA-B*51:01 among these cohorts. Another possibility is that this mutation is selected by HIV-1-specific CTLs restricted by other HLA alleles, which are highly frequent among Japanese individuals but infrequent in or absent from other populations. To clarify the latter possibility, we first analyzed the association of the I135X mutation with other HLA class I alleles in a Japanese cohort and found this mutation also to be associated with HLA-B*52:01. We next sought to identify an HLA-B*52:01-restricted CTL epitope including RT135 and found that both HLA-B*51:01 and -B*52:01 can present the same epitope, Pol283-8. Using population level analyses of Japanese and Caucasian cohorts, we identified HLA-B*51:01- and HLA-B*52:01-specific polymorphisms at RT codon 135 (position 8 of this epitope) and characterized differential pathways of escape between these two alleles. In addition, we assessed the *in vitro* ability of HLA-B*52:01- and HLA-B*51:01-restricted CTLs to se-

Received 20 September 2012 Accepted 26 November 2012
Published ahead of print 12 December 2012
Address correspondence to Masafumi Takiguchi, masafumi@kumamoto-u.ac.jp.
Y.Y., N.K., and K.K. contributed equally to this study.
Supplemental material for this article may be found at http://dx.doi.org/10.1128/JVI.02572-12.

doi:10.1128/JVI.02572-12

lect I135X mutants and elucidated the crystal structure of the HLA-B*52:01-Pol283-8 peptide complex.

MATERIALS AND METHODS

Patients. Two hundred fifty-seven chronically HIV-1-infected, antiretroviral-naïve Japanese individuals were recruited for the present study, which was approved by the ethics committees of Kumamoto University and the National Center for Global Health and Medicine, Japan. Written informed consent was obtained from all subjects according to the Declaration of Helsinki.

In addition, HLA-associated immune selection pressure at RT codon 135 was investigated in the International HIV Adaptation Collaborative (IHAC) cohort, comprising >1,200 chronically HIV-infected, antiretroviral-naïve individuals from Canada, the United States, and Western Australia (19). The majority of the IHAC participants were Caucasian, and the HIV subtype distribution was >95% subtype B.

HIV-1 clones. An infectious proviral clone of HIV-1, pNL-432, and its mutant form pNL-M20A (containing a substitution of Ala for Met at residue 20 of Nef) were previously reported (29). Pol283-8 mutant viruses (Pol283-8L, -8T, -8V, and 8R) were previously generated on the basis of pNL-432 (15, 28).

Generation of CTL clones. Pol283-8-specific, HLA-B*52:01-restricted CTL clones were generated from HIV-1-specific, bulk-cultured T cells by limiting dilution in U-bottom 96-well microtiter plates (Nunc, Roskilde, Denmark). Each well contained 200 μl of the cloning mixture (about 1×10^6 irradiated allogeneic peripheral blood mononuclear cells (PBMCs) from healthy donors and 1×10^5 irradiated C1R-B*52:01 cells prepulsed with the corresponding peptide at 1 μM in RPMI 1640 supplemented with 10% human plasma and 200 U/ml human recombinant interleukin-2).

Intracellular cytokine staining (ICS) assay. PBMCs from HIV-1-seropositive HLA-B*52:01$^+$ HLA-B*51:01$^-$ individuals were cultured with each peptide (1 μM). Two weeks later, the cultured cells were stimulated with C1R-B*52:01 cells or those prepulsed with Pol283-8 peptide (1 μM) for 60 min, and then they were washed twice with RPMI 1640 containing 10% fetal calf serum (RPMI 1640-10% FCS). Subsequently, brefeldin A (10 μg/ml) was added. After these cells had been incubated for 6 h, they were stained with an anti-CD8 monoclonal antibody (MAb; Dako Corporation, Flostrup, Denmark), fixed with 4% paraformaldehyde, and then permeabilized with permeabilization buffer. Thereafter, the cells were stained with an anti-gamma interferon (IFN-γ) MAb (BD Bioscience). The percentage of CD8$^+$ cells positive for intracellular IFN-γ was analyzed by using a FACS-Cant II (BD Biosciences, San Jose, CA). All flow cytometric data were analyzed with FlowJo software (Tree Star, Inc., Ashland, OR).

Identification of 11-mer peptide recognized by HLA-B*52:01-restricted CD8$^+$ T cells. We identified an 11-mer peptide recognized by HLA-B*52:01-restricted CD8$^+$ T cells as follows. We stimulated PBMCs from a chronically HIV-1-infected HLA-B*52:01$^+$ donor (KI-069) with a peptide cocktail including overlapping 17-mer peptides covering RT135 and cultured the cells for 14 days. The cells in bulk culture were assessed by performing an ICS assay for C1R-HLA-B*52:01 cells prepulsed with each of these 17-mer peptides. The bulk-cultured cells recognized the target cells prepulsed with two of the 17-mer peptides assessed, Pol17-47 (KDFRKYTAFTIPSINNE) and Pol17-48 (TAFTIPSI NNETPGIRT). Further analysis with 11-mer overlapping peptides covering the Pol17-48 sequence showed that these bulk-cultured cells recognized the target cells prepulsed with Pol11-142 (TAFTIPSINNE) but not those prepulsed with Pol11-143 (FTIPSINNETP).

Assay of cytotoxicity of CTL clones to target cells prepulsed with the epitope peptide or infected with a vaccinia virus–HIV-1 recombinant. The cytotoxicity of Pol283-8-specific, HLA-B*52:01-restricted CTL clones to C1R cells expressing HLA-B*52:01 (C1R-B*52:01), which were previously generated (30), and prepulsed with peptide or infected with a vaccinia virus-HIV-1Gag/Pol recombinant was determined by the standard ^{51}Cr release assay described previously (31). In brief, the infected cells were incubated with 150 μCi $Na_2{}^{51}CrO_4$ in saline for 60 min and then washed three times with RPMI 1640 medium containing 10% newborn calf serum. Labeled target cells (2×10^3/well) were added to each well of a U-bottom 96-well microtiter plate (Nunc, Roskilde, Denmark) with the effector cells at an effector-to-target (E/T) cell ratio of 2:1. The cells were then incubated for 6 h at 37°C. The supernatants were collected and analyzed with a gamma counter. Spontaneous ^{51}Cr release was determined by measuring the number of counts per minute (cpm) in supernatants from wells containing only target cells (cpm spn). Maximum ^{51}Cr release was determined by measuring the cpm in supernatants from wells containing target cells in the presence of 2.5% Triton X-100 (cpm max). Specific lysis was defined as (cpm exp − cpm spn)/(cpm max − cpm spn) × 100, where cpm exp is the number of cpm in the supernatant in the wells containing both target and effector cells.

Enzyme-linked immunospot (ELISPOT) assay. Cryopreserved PBMCs of chronically HIV-1-infected HLA-B*52:01$^+$ individuals were plated in 96-well polyvinylidene plates (Millipore, Bedford, MA) that had been precoated with 5 μg/ml anti-IFN-γ MAb 1-DIK (Mabtech, Stockholm, Sweden). The appropriate amount of each peptide (100 or 10 nM) was added in a volume of 50 μl, and then PBMCs were added at 1×10^5 cells/well in a volume of 100 μl. The plates were incubated for 40 h at 37°C in 5% CO_2 and then washed with phosphate-buffered saline (PBS) before the addition of biotinylated anti-IFN-γ MAb (Mabtech) at 1 μg/ml. After the plates had been incubated at room temperature for 100 min and then washed with PBS, they were incubated with streptavidin-conjugated alkaline phosphatase (Mabtech) for 40 min at room temperature. Individual cytokine-producing cells were detected as dark spots after a 20-min reaction with 5-bromo-4-chloro-3-indolylphosphate and nitroblue tetrazolium by using an alkaline phosphatase-conjugate substrate (Bio-Rad, Richmond, CA). The spots were counted by an Eliphoto-Counter (Minerva Teck, Tokyo, Japan). PBMCs without peptide stimulation were used as a negative control. Positive responses were defined as those greater than the mean of the negative-control wells plus 2 standard deviations (SD) (the number of spots in wells without peptides).

HIV-1 replication suppression assay. The ability of HIV-1-specific CTLs to suppress HIV-1 replication was examined as previously described (32). CD4$^+$ T cells isolated from PBMCs derived from an HIV-1-seronegative individual with HLA-B*52:01, HLA-B*51:01, or both were cultured. After the cells had been incubated with the desired HIV-1 clones for 4 h at 37°C, they were washed three times with RPMI 1640-10% FCS medium. The HIV-1-infected CD4$^+$ T cells were then cocultured with Pol283-8-specific CTL clones. From day 3 to day 7 postinfection, culture supernatants were collected and the concentration of p24 antigen (Ag) in them was measured by use of an enzyme-linked immunosorbent assay kit (HIV-1 p24 Ag ELISA kit; ZeptoMetrix).

HLA stabilization assay with RMA-S cells expressing HLA-B*52:01 or HLA-B*51:01. The peptide-binding activity of HLA-B*52:01 or HLA-B*51:01 was assessed by performing an HLA stabilization assay with RMA-S cells expressing HLA-B*52:01 (RMA-S-B*52:01) or HLA-B*51:01 (RMA-S-B*51:01) as described previously (33). Briefly, RMA-S-B*51:01 and RMA-S-B*52:01 cells were cultured at 26°C for 16 to 24 h. The cells (2×10^5) in 50 μl of RPMI 1640 supplemented with 5% FCS (RPMI–5% FCS) were incubated at 26°C for 3 h with 50 μl of a solution of peptides at 10^{-3} to 10^{-7} M and then at 37°C for 3 h. After having been washed with RPMI–5% FCS, the cells were incubated for 30 min on ice with an appropriate dilution of TP25.99 MAb. After two washings with RPMI–5% FCS, they were incubated for 30 min on ice with an appropriate dilution of fluorescein isothiocyanate (FITC)-conjugated anti-mouse Ig antibodies. Finally, the cells were washed three times with RPMI–5% FCS and the fluorescence intensity of the cells was measured by the FACS-Cant II. Relative mean fluorescence intensity (MFI) was calculated by subtracting the MFI of cells not peptide pulsed from that of the peptide-pulsed ones.

Sequencing of plasma RNA. Viral RNA was extracted from the plasma of chronically HIV-1-infected Japanese individuals by using a QIAamp

Mini Elute Virus spin kit (Qiagen). cDNA was synthesized from the RNA with Superscript II and random primer (Invitrogen). We amplified HIV RT and integrase sequences by nested PCR with RT-specific primers 5′-CCAAAAGTTAAGCAATGGCC-3′ and 5′-CCCATCCAAAGGAATGG AGG-3′ or 5′-CCTTGCCCCTGCTTCTGTAT-3′ for the first-round PCR and 5′-AGTTAGGAATACCACACCCC-3′ and 5′-GTAAATCCCC ACCTCAACAG-3′ or 5′-AATCCCCACCTCAACAGAAG-3′ for the second-round PCR and integrase-specific primers 5′-ATCTAGCTTTGCAG GATTCGGG-3′ and 5′-CCTTAACCGTAGTACTGGTG-3′ or 5′-CCTG ATCTCTTACCTGTCC-3′ for the first-round PCR and 5′-AAAGGTCT ACCTGGCATGGG-3′ or 5′-TTGGAGAGCAATGGCTAGTG-3′ and 5′-AGTCTACTTGTCCATGCATGGC-3′ for the second-round PCR. PCR products were sequenced directly or cloned with a TOPO TA cloning kit (Invitrogen) and then sequenced. Sequencing was done with a BigDye Terminator v1.1. cycle sequencing kit (Applied Biosystems) and analyzed by an ABI PRISM 310 Genetic Analyzer.

Statistical analysis with phylogenetically corrected odds ratios. Strength of selection was measured by using a phylogenetically corrected odds ratio as previously described (19). Briefly, the odds of observing a given amino acid (e.g., 135V) was modeled as $P/(1 - P) = (a \times X) + (b \times T)$, where P is the probability of observing 135V in a randomly selected individual, X is a binary (0/1) variable representing whether or not an individual expresses the HLA allele in question (e.g., B*52:01), and T equals 1 if the transmitted/founder virus for that individual carried 135V and −1 otherwise. Because the transmitted/founder virus is unknown, we averaged over all possibilities by using weights informed by a phylogeny that was constructed from the RT sequences of all of the individuals in the study. The parameters a and b were determined by using iterative maximum-likelihood methods. The maximum-likelihood estimate of a is an estimate of the natural logarithm of the odds ratio of observing 135V in individuals expressing X versus individuals not expressing X, conditioned on the individuals' (unobserved) transmitted/founder virus. P values are estimated by using a likelihood ratio test that compares the above model to a null model in which a equals 0.

To compare the odds of selection between two cohorts, we modified the phylogenetically corrected logistic regression model to include a cohort term, $Z = X \times Y$, where X is the HLA allele, and Y is a 0/1 variable that indicates cohort membership, yielding $P/(1 - P) = (a \times X) + (b \times T) + (c \times Z)$, as previously described (19, 34). A P value testing if the odds of escape are different in the two cohorts was estimated by using a likelihood ratio test that compared this model to a null model where c equals 0.

Generation of HLA class I tetramers. HLA class I-peptide tetrameric complexes (tetramer) were synthesized as described previously (31, 35). The Pol283-8 peptide was used for the refolding of HLA-B*51:01 or HLA-B*52:01 molecules. Phycoerythrin (PE)-labeled streptavidin (Molecular Probes) was used for generation of the tetramers.

Tetramer binding assay. HLA-B*51:01-restricted and HLA-B*52:01-restricted CTL clones were stained at 37°C for 30 min with PE-conjugated HLA-B*51:01-tetramer and HLA-B*52:01-tetramer, respectively, at concentrations of 5 to 1,000 nM. After two washes with RPMI 1640 medium supplemented with 10% FCS (RPMI 1640–10% FCS), the cells were stained with FITC-conjugated anti-CD8 MAb at 4°C for 30 min, followed by 7-amino-actinomycin D at room temperature for 10 min. After two more washes with RPMI 1640–10% FCS, the cells were analyzed by the FACS-Cant II flow cytometer. The tetramer concentration that yielded the half-maximal MFI (the EC_{50}) was calculated by probit analysis.

Crystallization, data collection, and structure determination. Soluble HLA-B*52:01 (with beta-2 microglobulin and peptide TAFTIPSI) was prepared as described above. Prior to crystallization trials, HLA-B*52:01 was concentrated to a final concentration of 20 mg ml^{-1} in 20 mM Tris-HCl (pH 8.0) buffer containing 250 mM NaCl. This was done with a Millipore centrifugal filter device (Amicon Ultra-4, 10-kDa cutoff; Millipore). Screening for crystallization was performed with commercially available polyethylene glycol (PEG)-based screening kits, PEGs and PEGs II suites (Qiagen). Thin needle crystals were observed from PEGs II suite 23 (0.2 M sodium acetate, 0.1 M HEPES [pH 7.5], and 20% PEG 3000). Several conditions were further screened by the hanging-drop method with 24-well VDX plates (Hampton Research) by mixing 1.5 μl protein solution and 1.5 μl reservoir to be equilibrated against reservoir solution (0.5 ml) at 293 K. Best crystals were grown from macro seeding with the initial crystals obtained with 0.2 M sodium acetate, 0.1 M Bis Tris propane [pH 7.5], and 20% PEG 3350.

The data set was collected at beamline BL41XU of SPring-8 with Rayonix charge-coupled device detector MX225HE. Prior to diffraction data collection, crystals were cryoprotected by transfer to a solution containing 25% (vol/vol) glycerol and incubation in it for a few seconds, followed by flash cooling. The data sets were integrated with XDS (36) and then merged and scaled by using Scala (37). HLA-B*52:01 crystals belonged to space group $P2_12_12_1$, with unit cell parameters $a = 69.0$ Å, $b = 83.3$ Å, and $c = 170.3$ Å. Based on the values of the Matthews coefficient (V_M) (38), we estimated that there were two protomers in the asymmetric unit with a V_M value of 1.37 A^3/Da (Vsolv = 10.5%). For details of the data collection and processing statistics, see Table S1 in the supplemental material.

The structure was solved by the molecular replacement method with Molrep (39). The crystal structure of HLA-B*51:01 (PDB ID: 1E28) was used as a search model. Structure refinement was carried out by using Refmac5 (40) and phenix (41). The final model was refined to an Rfree factor of 34.7% and an R factor of 29.5% with a root mean square deviation of 0.014 Å in bond length and 1.48° in bond angle for all reflections between resolutions of 38.8 and 3.1 Å. Table S1 in the supplemental material also presents a summary of the statistics for structure refinement. The stereochemical properties of the structure were assessed by Procheck (42) and COOT (43) and showed no residues in the disallowed region of the Ramachandran plot.

Protein structure accession number. Atomic coordinates and structure factors for HLA-B*52:01 have been deposited in the Protein Data Bank under accession code 3W39.

RESULTS

Association of I135X variants with HLA-B*52:01. To clarify the possibility that CTLs restricted by other HLA alleles select the I135X mutation, we investigated the association between other HLA alleles and this mutation in 257 Japanese individuals chronically infected with HIV-1. We found an association of HLA-B*52:01 with the I135X variant, though this association was weaker than that with HLA-B*51:01 (phylogenetically corrected ln odds ratio [lnOR] of 11.76 [$P = 8.77 \times 10^{-4}$] for B*52:01 versus an lnOR of 40.0 [$P = 5.78 \times 10^{-12}$] for B*51:01; Table 1). We also analyzed the effects of HLA-B*52:01 and HLA-B*51:01 in chronically HIV-1-infected Japanese individuals, excluding HLA-B*51:01$^+$ and HLA-B*52:01$^+$ individuals, respectively, and found a significant association between HLA-B*52:01 and I135X variants among 200 HLA-B*51:01-negative individuals with chronic HIV-1 infection ($P = 4.7 \times 10^{-4}$; see Fig. S1A in the supplemental material) and that of HLA-B*51:01 with the variants in 202 HLA-B*52:01-negative ones ($P = 5.3 \times 10^{-8}$; see Fig. S1B in the supplemental material). These results together imply that HLA-B*52:01-restricted CTLs selected this mutation.

Identification of HLA-B*52:01-restricted, Pol283-specific CTLs. To identify the HLA-B*52:01-restricted HIV-1 epitope including RT135, we first investigated whether overlapping peptides covering RT135 could elicit CD8$^+$ T cells specific for these peptides in chronically HIV-1-infected individuals. We identified CTLs recognizing the Pol11-142 (TAFTIPSINNE) peptide in a chronically HIV-1-infected HLA-B*52:01$^+$ donor, KI-069 (see Materials and Methods). Since the C terminus of HLA-B*52:01-binding peptides is known to be a hydrophobic residue (30, 44), we speculated that TAFTIPSI (Pol283-8) was the epitope peptide.

TABLE 1 HLA-B*52:01 and HLA-B*51:01 association with variation at RT135 in Japanese and Caucasian cohorts

HLA class I allele	RT135 target variable	PlyloLOR[a]		Within-cohort *P* value		*P* value comparing cohorts
		Japanese	IHAC	Japanese	IHAC	
B*51:01	T	13.70	4.53	4.66×10^{-6}	1.70×10^{-35}	0.042
B*52:01	T	−9.77	1.25	0.464	2.04×10^{-3}	0.62
B*51:01	I	−40.00	−5.71	5.78×10^{-12}	1.58×10^{-51}	0.052
B*52:01	I	−11.76	−3.06	8.77×10^{-4}	2.95×10^{-5}	0.52
B*51:01	V	−9.76	8.52	0.884	0.41	0.85
B*52:01	V	12.21	10.15	0.076	1.82×10^{-3}	0.037
B*51:01	R	12.08	13.02	0.038	2.36×10^{-3}	0.42
B*52:01	R	0.26	8.37	0.423	0.469	0.89
B*51:01	L	−0.89	3.21	1	0.038	0.17
B*52:01	L	−0.56	3.61	1	0.231	0.29
B*51:01	K	−0.71	−40.00	1	0.53	0.99
B*52:01	K	−0.69	−40.00	1	0.779	0.99
B*51:01	M	7.76	12.00	0.894	2.10×10^{-4}	0.34
B*52:01	M	11.09	−40.00	0.034	0.517	0.12

[a] PlyloLOR, phylogenetically corrected lnOR.

Indeed, bulk-cultured T cells that had been cultured for 2 weeks after stimulation with Pol17-48 recognized C1R-B*52:01 cells prepulsed with Pol283-8 peptide at a much lower concentration than those incubated with the Pol11-142 peptide (Fig. 1A), strongly suggesting that Pol283-8 is an epitope recognized by HLA-B*52:01-restricted CTLs. These findings were confirmed by ELISPOT assay with PBMCs from two HLA-B*52:01$^+$ individuals chronically infected with HIV-1 (Fig. 1B). To clarify whether this peptide was processed and presented by HLA-B*52:01, we investigated the killing activity of bulk-cultured T cells against HLA-B*52:01$^+$ target cells infected with a vaccinia virus–HIV-1 Gag/Pol recombinant. They killed target cells infected with this recombinant but not those infected with wild-type vaccinia virus (Fig. 1C), indicating that the Pol283-8 peptide was presented by

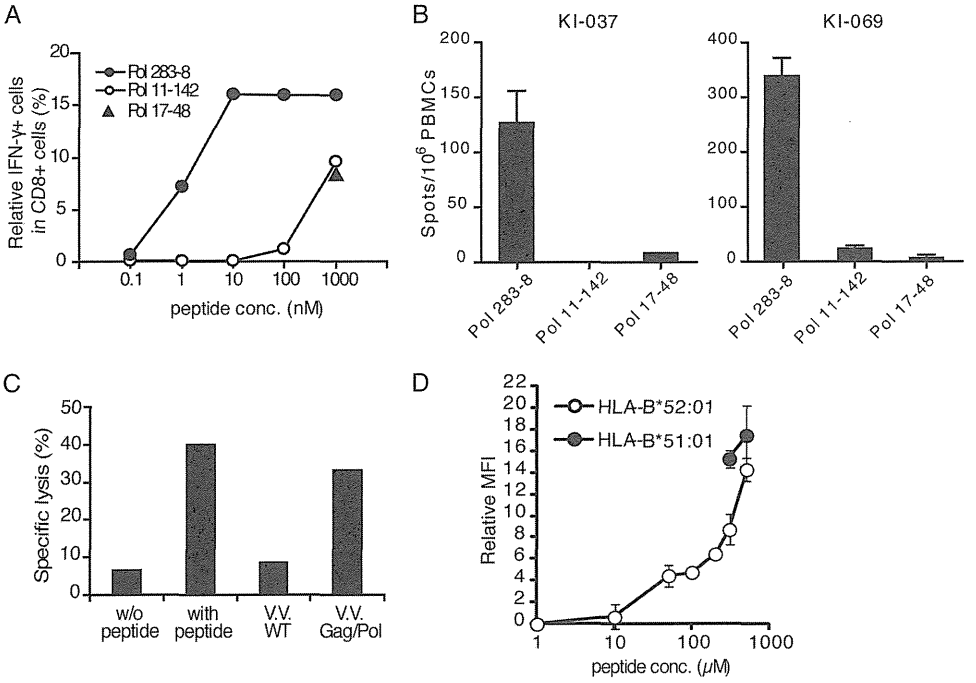

FIG 1 Identification of HLA-B*52:01-restricted Pol epitope. (A) Identification of the epitope peptide recognized by HLA-B*52:01-restricted CD8$^+$ T cells. Bulk T cells were cultured for 2 weeks after stimulation with the Pol17-48 peptide, and then the recognition of C1R-HLA-B*52:01 cells prepulsed with Pol17-48, Pol11-142, or Pol283-8 peptide was assessed by ICS assay. (B) Pol283-8 peptide recognition by T cells *ex vivo*. Recognition of the Pol17-48, Pol11-142, or Pol283-8 peptide by PBMCs from two HLA-B*52:01$^+$ individuals chronically infected with HIV-1 (KI-037 and KI-069) was analyzed by ELISPOT assay. A 100 nM concentration of each peptide was used. (C) Killing activity of Pol283-specific, HLA-B*52:01-restricted CD8$^+$ T cells against cells infected with a vaccinia virus–HIV-1 Gag/Pol recombinant. The killing activities of bulk-cultured T cells stimulated with Pol11-142 against target cells infected with a vaccinia virus–HIV-1 Gag/Pol recombinant (Gag/Pol) and against those infected with wild-type vaccinia virus (V.V. WT) are shown. (D) Binding of Pol283-8 peptide to HLA-B*52:01. Binding ability was measured by performing the HLA class I stabilization assay with RMA-S-B*52:01. RMA-S-B*51:01 cells were used as control cells for the Pol283-8 peptide.

TABLE 2 Pol283-8-specific CD8$^+$ T cells in chronically HIV-1-infected, HLA-B*52:01$^+$ individuals

Patient ID	HLA class I alleles		No. of CD4 cells/μl	No. of CD8 cells/μl	Viral load (no. of copies/ml)	Antiretroviral therapy	Relative IFN-γ$^+$/CD8$^+$ % in ICC assay	No. of spots/10^6 PBMCs in ELISPOT[a] assay
KI-037	A*24:02/−	B*52:01/40:02	465	973	76,000	−	64.1	150
KI-090	A*24:02/−	B*52:01/55:01	606	511	≤50	+	40.2	80
KI-106	A*24:02/33:03	B*52:01/07:01	433	890	≤50	+	1.4	<79
KI-126	A*24:02/31:01	B*52:01/40:01	465	NT[b]	36,000	−	60.4	<79
KI-130	A*24:02/−	B*52:01/07:02	351	1,275	14,000	−	0.0	<79
KI-167	A*24:02/−	B*52:01/54:01	455	909	26,000	−	0.0	<79
KI-067	A*24:02/−	B*52:01/48:01	234	1,198	89,000	−	10.9	<79
KI-071	A*24:02/31:01	B*52:01/40:06	292	1,134	48,000	−	0.7	<79
KI-076	A*02:01/24:01	B*52:01/40:01	136	252	14,000	−	61.0	80
KI-114	A*02:01/24:01	B*52:01/27:04	416	463	≤50	+	0.1	<79
KI-056	A*24:02/−	B*52:01/40:02	290	844	8,200	−	-0.1	<79
KI-108	A*24:02/−	B*52:01/−	373	481	NT	−	1.0	<79
KI-028	A*24:02/26:01	B*52:01/48:01	1,351	811	≤50	+	0.5	<79
KI-069	A*24:02/−	B*52:01/40:06	448	1,631	4,400	−	18.1	790

[a] More than the mean number of negative-control spots + 2 SD was defined as a positive response (positive response, >79 spots).
[b] NT, not tested.

HLA-B*52:01. We analyzed the binding of the Pol283-8 peptide to HLA-B*52:01 by using the HLA stabilization assay. The results demonstrated that this peptide bound to HLA-B*52:01 (Fig. 1D). These results together indicate that the Pol283-8 epitope can therefore be presented by both HLA-B*51:01 and HLA-B*52:01.

We investigated whether Pol283-8-specific CD8$^+$ T cells were elicited predominantly in chronically HIV-1-infected HLA-B*52:01$^+$ HLA-B*51:01$^-$ individuals. PBMCs from 14 of these individuals were analyzed by ICS assay with Pol283-8 peptide-stimulated culture cells, as well as by ELISPOT assay. The results of the ICS assay showed that 7 of these 14 HLA-B*52:01$^+$ HLA-B*51:01$^-$ patients had Pol283-specific CD8$^+$ T cells, whereas those of the ELISPOT assay with *ex vivo* PBMCs revealed that Pol283-specific CD8$^+$ T cells were detected in only four individuals (Table 2). These results suggest that the three individuals in whom the specific CTLs were detected by the ICS assay but not by the ELISPOT assay may have memory T cells. These results together indicate that Pol283-8 was recognized as an HLA-B*52:01-restricted immunodominant epitope in the HLA-B*52:01$^+$ individuals and support the idea that the I135X mutation was selected by HLA-B*52:01-restricted, Pol283-8-specific CD8$^+$ T cells.

Strong ability of HLA-B*52:01-restricted, Pol283-8-specific CD8$^+$ T cells to suppress HIV-1 replication. A previous study showed that HLA-B*51:01-restricted, Pol283-8-specific T cells have a strong ability to kill HIV-1-infected target cells and to suppress HIV-1 replication (31). Therefore, we expected that the HLA-B*52:01-restricted T cells also would have this strong ability. We generated HLA-B*52:01-restricted, Pol283-8-specific T cell clones and investigated their ability to kill peptide-pulsed or HIV-1-infected target cells. Clone 1E1 effectively killed C1R-B*52:01 cells prepulsed with the Pol283-8 peptide (Fig. 2A) and NL-432-infected CD4$^+$ T cells from an HLA-B*52:01$^+$ individual (Fig. 2B). Additional T cell clones also showed strong killing activity against NL-432-infected HLA-B*52:01$^+$ CD4$^+$ T cells (data not shown). In addition, we investigated the ability of these CTL clones to suppress HIV-1 replication. CD4$^+$ T cells derived from an HLA-B*52:01$^+$ individual were infected with NL-432 or M20A mutant virus, the latter of which has an amino acid substitution at position 20 of Nef and lacks the ability to downregulate the surface expression of HLA-A and -B molecules (Fig. 2C). Representative data on the 1E1 clone and summary data on four clones are shown in Fig. 2D and E, respectively. These CTL clones strongly suppressed the replication of both the NL432 and M20A mutant viruses, indicating that the HLA-B*52:01-restricted CTLs had a strong ability to suppress HIV-1 replication, as was the case with the HLA-B*51:01-restricted ones.

Recognition of I135X mutations by Pol283-8-specific, HLA-B*52:01-restricted CTLs. Four mutations (8T, 8L, 8R, and 8V) were observed predominantly at RT135 in chronically HIV-1-infected HLA-B*52:01$^+$ individuals (Fig. 3). These mutations may have been selected by Pol283-8-specific, HLA-B*52:01-restricted CTLs in these patients. We therefore investigated the ability of HLA-B*52:01-restricted CTLs to suppress the replication of these mutant viruses *in vitro*. The CTL clones failed to suppress the replication of the 8L, 8T, or 8R mutant, though they weakly suppressed that of the 8V virus at an E/T cell ratio of 1:1 (Fig. 4A). These results support the idea that these variants were escape mutations from the HLA-B*52:01-restricted CTLs. To clarify the mechanism by which the CTL clones failed to suppress the replication of these mutant viruses, we investigated the CTL clones for recognition of C1R-B*52:01 cells prepulsed with the mutant peptides. The CTL clones effectively recognized the 8V peptide at the same level as the wild-type peptide and the 8T and 8L peptides at less than that of the wild-type one, whereas they failed to recognize the 8R peptide (Fig. 4B). An ELISPOT assay with *ex vivo* PBMCs from KI-069 showed that Pol283-8-specific CTLs effectively recognized the 8I and 8V variants but not the other three mutant peptides (Fig. 4C), suggesting that Pol283-8-specific CTLs failed to recognize the 8T, 8L, and 8R peptides *in vivo*. The lack of recognition of these mutants by CTLs may be attributable to a failure of T cell receptor (TCR) recognition, the inability of the peptide to bind to HLA-B*52:01, and/or disruption of the processing of the epitope in HIV-1-infected cells.

Different pattern of RT135 mutation selection by two HLA alleles. As described above, HLA-B*51:01 and HLA-B*52:01 were associated with I135X in a Japanese population in which the prevalence of HLA-B*51:01 and B*52:01 alleles is relatively high (21.9 and 21.1%, respectively). In a Japanese cohort, out of the five

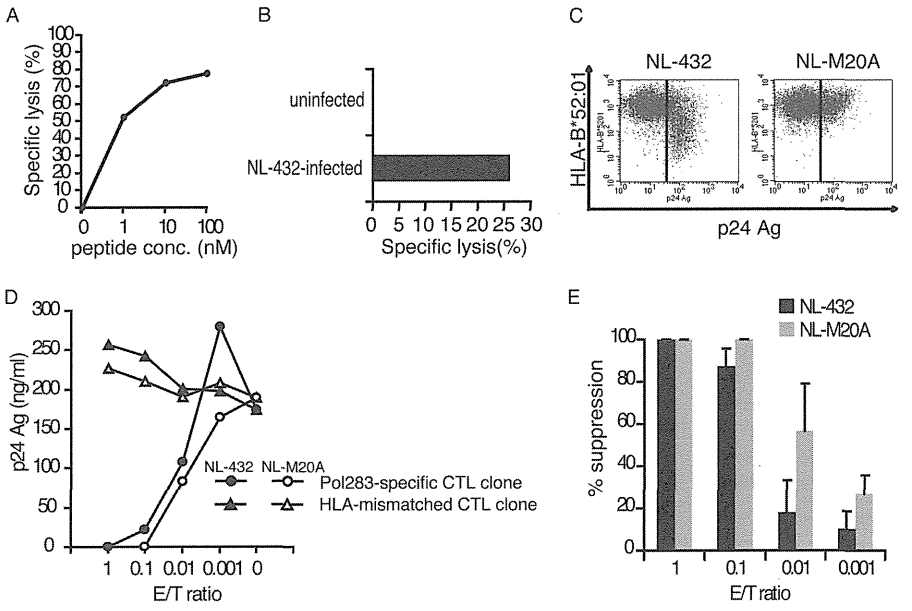

FIG 2 Abilities of HLA-B*52:01-restricted, Pol283-8-specific CD8$^+$ T cell clones to kill HIV-1-infected CD4$^+$ T cells and to suppress HIV-1 replication. (A) Killing activity of an HLA-B*52:01-restricted, Pol283-8-specific CD8$^+$ T cell clone against C1R-B*52:01 cells prepulsed with Pol283-8 peptides. The activity of an HLA-B*52:01-restricted, Pol283-8-specific CD8$^+$ T clone, 1E1, to kill C1R-B*52:01 cells was measured by performing a ^{51}Cr-release assay. (B) Killing activity of HLA-B*52:01-restricted, Pol283-8-specific CD8$^+$ T cell clone 1E1 against CD4$^+$ T cells infected with HIV-1. The ability of the clone to kill CD4$^+$ T cells infected with NL-432 was measured by performing a ^{51}Cr-release assay. (C) Downregulation of HLA-B*52:01 in HIV-1-infected CD4$^+$ T cells. CD4$^+$ T cells derived from an HLA-B*52:01$^+$ donor (HLA-A*11:01/A*24:02, HLA-B*52:01/B*52:01, and HLA-C*12:02/C*14:02) were infected with NL-432 and then cultured for 4 days. The cultured CD4$^+$ T cells were stained with anti-p24 Ag and TÜ109 anti-Bw4 MAbs. (D) Ability of an HLA-B*52:01-restricted, Pol283-8-specific CD8$^+$ T cell clone to suppress the replication of NL-432 and M20A mutant viruses. Suppressing ability was measured at four different E/T cell ratios (1:1, 0.1:1, 0.01:1, and 0.001:1). HIV-1-infected HLA-B*52:01$^+$ CD4$^+$ T cells were cocultured with an HLA-B*52:01-restricted, Pol283-8-specific CTL clone or an HLA-mismatched CTL clone at various E/T cell ratios. HIV-1 p24 Ag levels in the supernatant were measured on day 6 postinfection. (E) Summary of the ability of HLA-B*52:01-restricted, Pol283-8-specific CD8$^+$ T cell clones ($n = 4$) to suppress the replication of Nl-432 and M20A mutant viruses at four different E/T cell ratios.

amino acid mutations that can be generated by a one-nucleotide mutation from Ile, the T mutation was strongly associated with the presence of HLA-B*51:01 ($P = 4.66 \times 10^{-6}$), whereas HLA-B*52:01 was associated not with any single amino acid substitu-

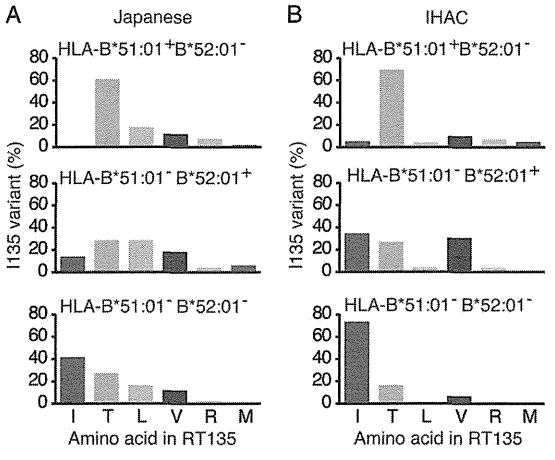

FIG 3 Amino acid variation at RT135 in Japanese individuals. (A) Frequency of the amino acid at RT135 in 51 HLA-B*51:01$^+$ HLA-B*52:01$^-$, 49 HLA-B*51:01$^-$ HLA-B*52:01$^+$, and 151 HLA-B*51:01$^-$ HLA-B*52:01$^-$ Japanese subjects. (B) Frequency of the amino acid at RT135 in 131 HLA-B*51:01$^+$ HLA-B*52:01$^-$, 26 HLA-B*51:01$^-$ HLA-B*52:01$^+$, and 1195 HLA-B*51:01$^-$ HLA-B*52:01$^-$ subjects in three predominantly Caucasian cohorts from Canada, the United States, and Western Australia (IHAC).

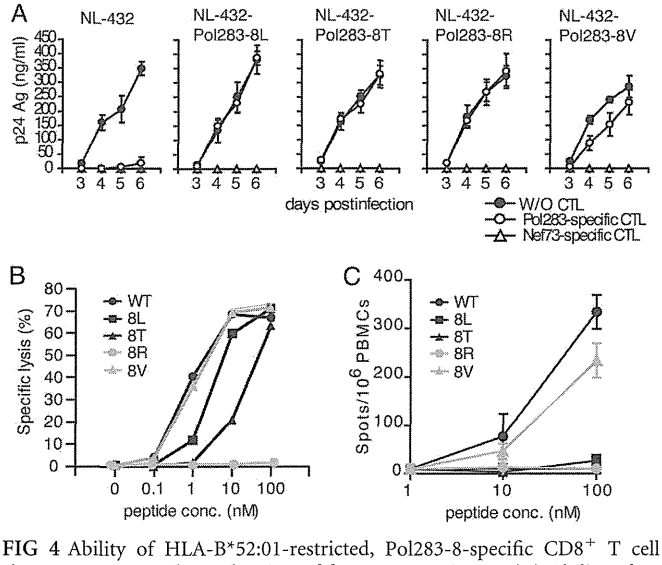

FIG 4 Ability of HLA-B*52:01-restricted, Pol283-8-specific CD8$^+$ T cell clones to suppress the replication of four mutant viruses. (A) Ability of an HLA-B*52:01-restricted, Pol283-8-specific CD8$^+$ T cell clone to suppress the replication of four (8L, 8T, 8R, and 8V) mutant viruses and NL-432. The abilities of an HLA-B*52:01-restricted, Pol283-8-specific CD8$^+$ T cell clone and an HLA-A*1101-restricted Nef73-specific T cell clone to suppress the replication of these viruses were measured at an E/T cell ratio of 1:1 on days 3 to 6. W/O, without. (B) Recognition by an HLA-B*52:01-restricted, Pol283-8-specific CD8$^+$ T cell clone of C1R-B*52:01 cells prepulsed with any one of the four mutant epitope peptides or the wild-type (WT) peptide (8I). (C) Recognition of mutant epitope peptides by *ex vivo* Pol283-8-specific CTLs. The recognition of the Pol283-8 peptide (WT) or the mutant epitope peptide by PBMCs from KI-069 was analyzed by ELISPOT assay.

tion but only with the non-I mutation ($P = 8.77 \times 10^{-4}$, Table 1). The distribution of amino acid variations at RT135 in the HLA-B*51:01$^+$ HLA-B*52:01$^-$ Japanese subjects was different from that in the HLA-B*51:01$^-$ HLA-B*52:01$^+$ ones (Fig. 3). These results suggest that the HLA-B*51:01-restricted CTLs strongly selected the 135T mutation but that the HLA-B*52:01-restricted ones selected a variety of different amino acids at this position in Japanese individuals.

We also analyzed the association of I135X mutations with HLA-B*52:01 and HLA-B*51:01 in three predominantly Caucasian cohorts from Canada, the United States, and Western Australia (International HIV Adaptation Collaborative [IHAC]) (19) comprising >1,200 subjects (Table 1). HLA-B*51:01 was very strongly associated with the I135X mutation (lnOR of 5.71; $P = 1.58 \times 10^{-51}$). Although only 2.1% of the IHAC cohort subjects expressed HLA-B*52:01, this allele was also associated with I135X (lnOR of 3.06; $P = 2.95 \times 10^{-5}$). The T mutation was strongly associated with HLA-B*51:01 ($P = 1.70 \times 10^{-35}$), whereas the T and V mutations were weakly associated with HLA-B*52:01 ($0.0005 < P < 0.005$). Thus, these results showed a similar selection of RT135 mutations by HLA-B*52:01 in the predominantly Caucasian cohort, despite a substantially lower frequency of HLA-B*52:01. The magnitude of the strength of selection by HLA-B*52:01 and HLA-B*51:01 on RT135 did not differ significantly between the two cohorts (Table 1). These results indicate that HLA-B*51:01 strongly selected 135T but that HLA-B*52:01 selected a variety of substitutions at this site (designated I135X) in both the Japanese and non-Japanese cohorts.

Comparison of TCR affinity and abilities of HLA-B*51:01-restricted and HLA-B*52:01-restricted CTLs to suppress HIV-1 replication. We investigated the TCR affinity of HLA-B*51:01-restricted and HLA-B*52:01-restricted CTL clones by using tetramers of the HLA-B*51:01-Pol283 peptide and the HLA-B*52:01-Pol283 peptide complex (HLA-B*51:01 and HLA-B*52:01 tetramers, respectively). The TCR affinity of these CTL clones was compared in terms of EC_{50}. The EC_{50} of the HLA-B*51:01-restricted CTL clones was significantly lower than that of the HLA-B*52:01-restricted CTL clones (Fig. 5A), suggesting that the former CTL clones had TCRs with a higher affinity for the ligand than those of the latter clones. These results imply that the HLA-B*51:01-restricted CTL clones could recognize the HIV-1-infected targets more effectively than HLA-B*52:01-restricted ones.

Since CD4$^+$ T cells derived from an HLA-B*52:01 homozygous individual were used in the experiment shown in Fig. 2D and E, the ability of the HLA-B*52:01-restricted CTL clones to suppress the replication of NL-432 may have been overestimated. To evaluate and compare the abilities of HLA-B*51:01-restricted and HLA-B*52:01-restricted CTL clones to suppress the replication of NL-432, we used CD4$^+$ T cells from individuals expressing HLA-B*51:01$^+$/B*52:01$^-$, HLA-B*51:01$^-$/B*52:01$^+$, or HLA-B*51:01$^+$/B*52:01$^+$ (Fig. 5B). Two HLA-B*51:01-restricted CTL clones strongly inhibited the replication of HIV-1 in cultures of NL-432-infected HLA-B*51:01$^+$/B*52:01$^-$ CD4$^+$ T cells but not in those of HLA-B*51:01$^-$/B*52:01$^+$ cells, whereas two HLA-B*52:01-restricted CTL clones strongly inhibited the replication of HIV-1 in cultures of NL-432-infected HLA-B*51:01$^-$/B*52:01$^+$ CD4$^+$ T cells but not in those of HLA-B*51:01$^+$/B*52:01$^-$ cells (Fig. 5B, left and middle). The ability of the HLA-B*51:01-restricted CTL clones to suppress the replication of HIV-1 was greater than that of the HLA-B*52:01-restricted CTL clones. This was confirmed by the experiment with HLA-B*51:01$^+$/B*52:01$^+$ CD4$^+$ T cells (Fig. 5B, right). Although both HLA-B*51:01-restricted and HLA-B*52:01-restricted CTL clones strongly inhibited the replication of HIV-1 in the cultures of NL-432-infected HLA-B*51:01$^+$/B*52:01$^+$ CD4$^+$ T cells, the former clones exhibited a greater ability to suppress the replication of HIV-1 than did the latter cells. These results indicate that the HLA-B*51:01-restricted CTL clones had a stronger ability to suppress HIV-1 replication than the HLA-B*52:01-restricted clones. Taken together, both our *in vitro* and our *in vivo* (population level HLA-association) data suggest that immune pressure on RT135 by HLA-B*51:01-restricted T cells was stronger than that imposed by HLA-B*52:01-restricted cells.

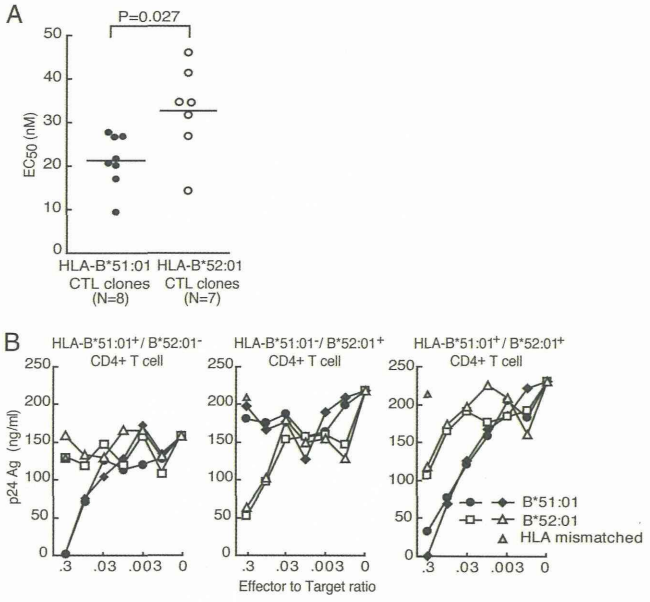

FIG 5 Differences between HLA-B*51:01-restricted and HLA-B*52:01-restricted CD8$^+$ T cell clones in TCR avidity and the ability to suppress HIV-1 replication. (A) TCR avidity of the HLA-B*51:01-restricted and HLA-B*52:01-restricted CTL clones expressed as EC_{50}. The ability of the TCRs of HLA-B*51:01-restricted and HLA-B*52:01-restricted CTL clones to bind HLA-B*51:01 tetramers and HLA-B*52:01 tetramers, respectively, was measured in terms of the MFI of each CTL clone stained with the tetramers at concentrations of 5 to 1,000 nM. (B) The ability of two HLA-B*51:01-restricted and two HLA-B*52:01-restricted CD8$^+$ T cell clones to suppress HIV-1 was measured at six different E/T cell ratios (0.3:1, 0.1:1, 0.03:1, 0.01:1, 0.003:1, and 0.001:1). CD4$^+$ T cells from individuals expressing HLA-B*51:01$^+$/B*52:01$^-$, HLA-B*51:01$^-$/B*52:01$^+$, or HLA-B*51:01$^+$/B*52:01$^+$ were infected with NL-432 and then cocultured with a given Pol283-8-specific CTL clone or an HLA-mismatched CTL clone. HIV-1 p24 Ag levels in the supernatant were measured on day 5 postinfection.

Structural basis of the difference in recognition between HLA-B*52:01- and HLA-B*51:01-restricted CTLs. In order to investigate the structural basis of the difference in recognition between HLA-B*52:01- and HLA-B*51:01-restricted CTLs, we performed a crystallographic study of the HLA-B*52:01 molecule complexed with the Pol283-8 peptide. The recombinant HLA-B*52:01 protein was crystallized, and by using the molecular replacement method, the three-dimensional structure of HLA-B*52:01 complexed with the Pol283-8 peptide was successfully determined. The crystal and statistical data are summarized in Table S1 in the supplemental material. The overall structure and peptide-binding mode were similar to those of HLA-B*51:01 complexed with the same Pol283-8 peptide (Fig. 6A and B), which

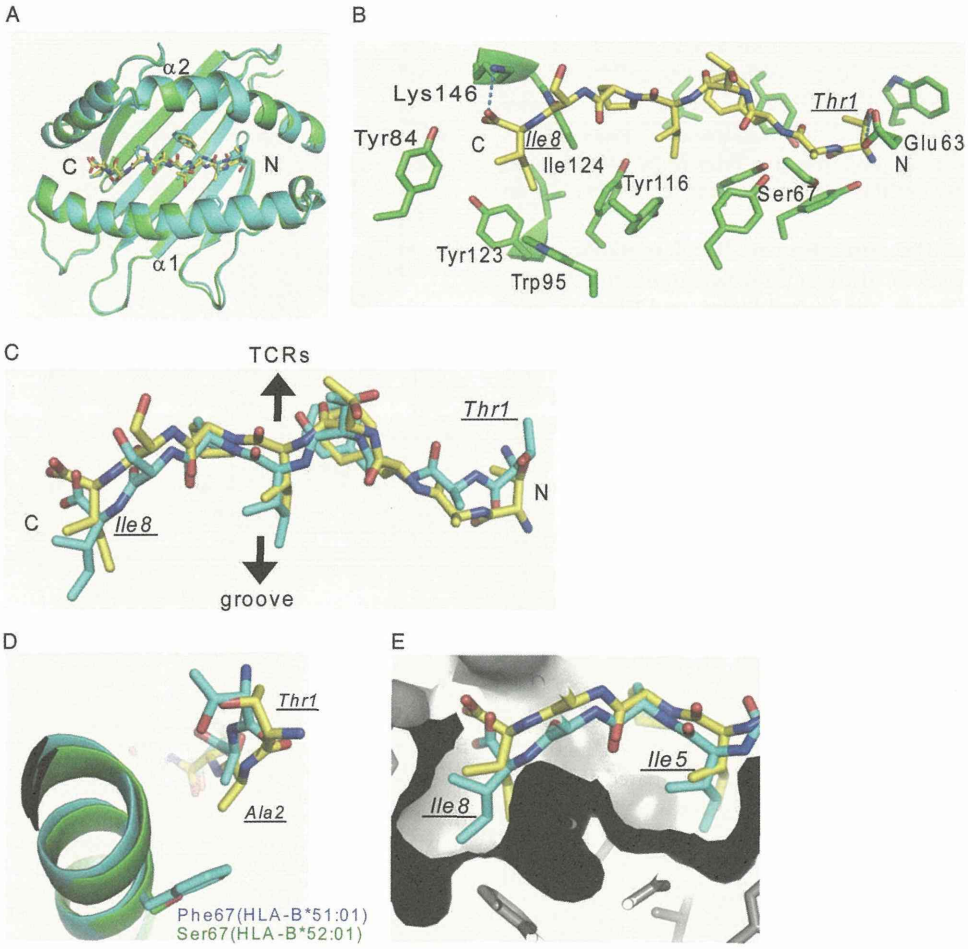

FIG 6 Structural comparison of HLA-B*52:01 and HLA-B*51:01 molecules complexed with the Pol283-8 peptide. (A) Crystal structures of HLA α1-α2 domains complexed with the Pol283-8 peptide (stick model) on the HLA-B*52:01 (green, yellow) and HLA-B*51:01 (cyan, cyan) complexes. This same coloring also applies to panels B to E. (B) Pol283-8 peptide and interacting side chains on the HLA-B*52:01 complex. Hydrogen bonds are shown as blue dotted lines. (C) Comparison of the Pol283-8 peptide conformations of HLA-B*52:01 and HLA-B*51:01 complexes. (D) N-terminal side of HLA-B*52:01 and HLA-B*51:01 complexes. (E) C-terminal side of HLA-B*52:01 and HLA-B*51:01 complexes. Surface presentation for the α1-α2 domains is shown in gray.

we had previously reported (45). This finding explains the cross presentation of this peptide by both HLA alleles. On the other hand, there was a notable conformational difference in the N-terminal region of the peptide between the two alleles (Fig. 6C and D). The replacement of Phe67 of HLA-B*51:01 with Ser in HLA-B*52:01 makes a local space, causing the N-terminal region of the peptide (T1 and A2) to reside deeper in the peptide-binding groove. Furthermore, the Gln63Glu mutation in HLA-B*52:01 affords a new interaction with the T1 residue of the peptide. These changes would, to some extent, have hidden the side chains of T1 and A2 (flat surface) from the TCRs, which may have reduced their interactions with TCRs on the HLA-B*52:01-restricted CTLs. On the other hand, the conformation of the C-terminal region of the peptide complexed with HLA-B*51:01 or HLA-B*52:01 was similar, even though C-terminal Ile8 of the peptide exhibited shallower penetration of the hydrophobic groove in the case of HLA-B*52:01 than in that of HLA-B*51:01 (Fig. 6C and E). These results may indicate that the relatively flat surface of the N-terminal side of the peptide contributed to the lower affinity for TCRs in the case of HLA-B*52:01.

DISCUSSION

HLA-B*52:01 and HLA-B*51:01 differ by only two residues, at positions 63 and 67 (44). Substitutions at these residues affect the formation of the B pocket in the peptide-binding pocket (45), suggesting the possibility that HLA-B*52:01 has a peptide motif different from that of HLA-B*51:01. Indeed, HLA-B*52:01-binding peptides have P2 primary anchors that are different from HLA-B*51:01-binding ones (30, 46). Since the Pol283-8 epitope carries Ala at its second position and Ile at the C terminus of the peptide, it is likely that this peptide would effectively bind to HLA-B*51:01 but not to HLA-B*52:01. However, the results of the HLA stabilization assay demonstrated that the Pol283-8 peptide did effectively bind to HLA-B*52:01. Since the HLA-B*52:01-binding peptide is known to have Pro as its preferred P2 anchor residue, this peptide carrying Ala at position 2 may be capable of binding to HLA-B*52:01. A previous study showed cross-recognition of alloreactive T cells between HLA-B*51:01 and HLA-B*52:01 (47, 48), indicating that some self-peptides can be presented by both of these HLA class I molecules. The findings on the crystal structure

TABLE 3 Numbers and frequencies of individuals having I135X mutations in a Japanese cohort and a predominantly Caucasian cohort

Cohort	No./total no. (%) of individuals				
	B*51:01$^+$ B*52:01$^-$	B*51:01$^-$ B*52:01$^+$	B*51:01$^+$ B*52:01$^+$	B*51:01$^-$ B*52:01$^-$	Total
Japanese	51/51 (100)	42/49 (85.7)	5/5 (100)	88/151 (58.3)	186/256 (72.6)
Caucasian	125/131 (95.4)	17/26 (65.4)	0/0	331/1,198 (27.6)	473/1,355 (34.9)

of the HLA-B*52:01 molecule complexed with the Pol283-8 peptide clarified that HLA-B*52:01 could bind to the peptide in a fashion similar to but slightly different from that of HLA-B*51:01. These findings support the presentation of the Pol283-8 peptide by both HLA-B*52:01 and HLA-B*51:01.

Pol283-8-specific CD8$^+$ T cells were detected in 7 of 14 HLA-B*52:01$^+$ HLA-B*51:01$^-$ individuals chronically infected with HIV-1. A previous analysis showed that CD8$^+$ T cells specific for this epitope are frequently detected in HLA-B*51:01$^+$ individuals chronically infected with HIV-1 (49). These results, taken together, indicate that this epitope is immunodominant in both HLA-B*51:01$^+$ and HLA-B*52:01$^+$ individuals. The analysis of 257 Japanese individuals revealed an association between HLA-B*52:01 and a variety of nonconsensus residues at RT codon 135 (I135X). Specifically, variants 8T, 8L, 8R, and 8V predominated in HLA-B*52:01$^+$ individuals, suggesting that these mutations had been selected by HLA-B*52:01-restricted CTLs. The viral suppression assay revealed that the HLA-B*52:01-restricted CTLs failed to suppress the replication of these mutant viruses. These results support the idea that the I135X mutation can be selected by immune pressure via Pol283-8-specific CTLs in HLA-B*52:01$^+$ individuals. Our previous studies showed that the 8L, 8T, and 8R mutations affected the recognition by Pol283-8-specific, HLA-B*51:01-restricted CTL clones (15, 28). These studies, together with the present study, indicate that accumulation of 8L, 8T, and 8R mutations in the HIV-infected Japanese population may be due to immune pressure by both HLA-B*52:01-restricted and HLA-B*51:01-restricted CTLs. Our analysis of the crystal structure of the HLA-B*52:01-peptide complex demonstrated that position 8 of the Pol283-8 peptide was deeply packed into the hydrophobic groove. Whereas the 8L, 8T, and 8R substitutions likely had a relatively large effect on the structure of the complex, the 8V mutation, resulting in only the deletion of the small methyl group, caused only very limited changes. Thus, the structural analysis supports the idea that the 8L, 8T, and 8R mutations affected the TCR recognition of the peptide and/or its binding to HLA-B*52:01.

The present study confirmed previous studies of nine worldwide cohorts (15) and a Chinese cohort (50) that showed a strong association of I135X with HLA-B*51:01. The I135X mutation was found in 58.3 and 27.6% of HLA-B*51:01$^-$ HLA-B*52:01$^-$ Japanese and predominantly Caucasian individuals, respectively (Table 3), supporting greater population level accumulation of this mutation in Japanese than in other cohorts. Since the Japanese cohort included twice as many HLA-B*51:01$^+$ individuals as the IHAC cohort (21.9% of Japanese and 9.4% of Caucasians in IHAC), the difference in the I135X variant frequency between these two cohorts would be driven, to a large extent, by the higher HLA-B*51:01 prevalence in the former than in the latter. The association of HLA-B*52:01 with this mutation was much weaker than that of HLA-B*51:01 in both cohorts but still highly statistically significant (an lnOR of 11.7 [$P = 8.77 \times 10^{-4}$] versus an lnOR of 40.0 [$P = 5.78 \times 10^{-12}$] in the Japanese cohort and an lnOR of 3.06 [$P = 2.95 \times 10^{-5}$] versus an lnOR of 5.71 [$P = 1.58 \times 10^{-51}$] in IHAC). Because of the relatively low B*52:01$^+$ frequency (~2%) in IHAC, the effect of HLA-B*52:01 on the overall prevalence of I135X was relatively low in this cohort. In contrast, in the Japanese cohort, where the HLA-B*52:01$^+$ prevalence was relatively high (>20%), this allele represents a major driving force behind 135X selection in this cohort. Thus, selection pressure from both HLA-B*51:01 and HLA-B*52:01 likely contributed to the observed population level accumulation of I135X mutations in the Japanese population.

Previous studies showed that HLA-B*51:01-restricted, Pol283-8-specific CTLs have a strong ability to suppress HIV-1 replication *in vitro* (28) and that they suppressed the replication of the 8V mutant virus but failed to suppress that of the 8T, 8L, and 8R mutant viruses (15). The frequency of the Pol283-8-specific CTLs was inversely correlated with the plasma viral load in HLA-B*51:01$^+$ hemophiliacs infected with HIV-1 approximately 30 years ago (28). The 8T, 8L, and 8R mutations did not affect replication capacity, whereas the 8V mutation conferred a modest fitness cost (15). These findings support the suppression of the wild-type or 8V mutant virus by Pol283-8-specific CTLs as a major mechanism of slow progression to AIDS in Japanese hemophiliacs. This CTL response was also elicited in Chinese HLA-B*51:01$^+$ individuals infected with the 8V mutant virus; furthermore, a low viral load and a high CD4 count were significantly associated with the presence of at least one of three HLA-B*51:01-restricted CTL responses, including a Pol283-8-specific one (50). Thus, these findings support the idea that Pol283-8-specific CTLs play an important role in the control of HIV-1 infection.

The present study demonstrated that HLA-B*52:01-restricted, Pol283-8-specific CTLs also had a strong ability to suppress HIV-1 replication *in vitro* (80% suppression at an E/T cell ratio of 0.3:1). However, the ability of HLA-B*52:01-restricted CTLs to suppress the replication of HIV-1 was weaker than that of HLA-B*51:01-restricted CTLs (Fig. 5B). Inspection of the crystal structures of both HLA molecules complexed with the Pol283-8 peptide suggests that the relatively shallow penetration of the hydrophobic groove of HLA-B*52:01 by the C-terminal side of the peptide, in contrast to the tightly packed binding with HLA-B*51:01, may have resulted in an unstable conformation of the complex. Furthermore, Ser67 of HLA-B*52:01 would have provided more space and loose interactions with the peptide than in the case of the Phe of HLA-B*51:01. Interestingly, the Pol283-8 peptide would have displayed only side chains of Thr1 and Ser7, and some part of the main chains, to CTLs. Therefore, these results suggest that the unstable backbone conformation and side chain positions in the case of HLA-B*52:01 largely contributed to the lower TCR affinity than that afforded by HLA-B*51:01. These results support that selection pressure *in vivo* via the HLA-B*52:01-restricted CTLs would be weaker than that via the HLA-B*51:01-restricted CTLs. Indeed, the prevalence of I135X mutations in HLA-B*51:

01^+ individuals was higher than that in HLA-B*52:01^+ individuals. The difference in the pattern of escape mutant selection by these CTLs between the HLA-B*51:01^+ and HLA-B*52:01^+ individuals might also have been due to the difference in their abilities to suppress HIV-1 replication. However, it still remains unclear why the 8T mutant was predominantly selected in the HLA-B*51:01^+ but not in the HLA-B*52:01^+ individuals. Further studies are expected to clarify the mechanism to explain how these CTLs selected different patterns of mutations at RT135.

Previous studies showed that the T242N mutant was selected by HLA-B*58:01-restricted and HLA-B*57-restricted CTLs specific for TW10 epitope in HIV-1 clade B-infected and clade C-infected individuals (25–27). Herein we also showed that I135X was selected by Pol283-8-specific CTLs restricted by two different HLA class I molecules. However, the strength and the pattern of the selection of I135X was different between HLA-B*51:01 and HLA-B*52:01. The present study suggests that this difference in the selection pattern was associated with that between the HLA-B*51:01^+ and HLA-B*52:01^+ individuals in terms of the ability of Pol283-specific CTLs to suppress HIV-1 replication. Thus, we characterized and experimentally validated distinct HIV-1 escape patterns of CTLs with the same epitope specificity and provided evidence that the extremely high prevalence of 135X in circulating Japanese sequences is likely driven not by one but by two HLA-B alleles.

ACKNOWLEDGMENTS

We thank Sachiko Sakai for her secretarial assistance, as well as Richard Harrigan and the BC Centre for Excellence in HIV/AIDS for data access. The assistance of Jennifer Listgarten and Carl Kadie (Microsoft Research) with HLA allele interpretation is also gratefully acknowledged.

N.K. is a JSPS Research Fellow. Z.L.B. is a recipient of a Canadian Institutes of Health Research (CIHR) New Investigator Award and a Michael Smith Foundation for Health Research (MSFHR) Scholar award. This research was supported by the Global COE program Global Education and Research Center Aiming at the Control of AIDS, launched as a project commissioned by the Ministry of Education, Science, Sports, and Culture, Japan, and by grants-in-aid for scientific research from the Ministry of Education, Science, Sports and Culture, Japan (18390141 and 20390134).

We have no financial conflicts of interest.

REFERENCES

1. **Borrow P, Lewicki H, Hahn BH, Shaw GM, Oldstone MB.** 1994. Virus-specific $CD8^+$ cytotoxic T-lymphocyte activity associated with control of viremia in primary human immunodeficiency virus type 1 infection. J. Virol. **68**:6103–6110.
2. **Koup RA, Safrit JT, Cao Y, Andrews CA, McLeod G, Borkowsky W, Farthing C, Ho DD.** 1994. Temporal association of cellular immune responses with the initial control of viremia in primary human immunodeficiency virus type 1 syndrome. J. Virol. **68**:4650–4655.
3. **Rinaldo C, Huang XL, Fan ZF, Ding M, Beltz L, Logar A, Panicali D, Mazzara G, Liebmann J, Cottrill M.** 1995. High levels of anti-human immunodeficiency virus type 1 (HIV-1) memory cytotoxic T-lymphocyte activity and low viral load are associated with lack of disease in HIV-1-infected long-term nonprogressors. J. Virol. **69**:5838–5842.
4. **Matano T, Shibata R, Siemon C, Connors M, Lane HC, Martin MA.** 1998. Administration of an anti-CD8 monoclonal antibody interferes with the clearance of chimeric simian/human immunodeficiency virus during primary infections of rhesus macaques. J. Virol. **72**:164–169.
5. **Ogg GS, Jin X, Bonhoeffer S, Dunbar PR, Nowak MA, Monard S, Segal JP, Cao Y, Rowland-Jones SL, Cerundolo V, Hurley A, Markowitz M, Ho DD, Nixon DF, McMichael AJ.** 1998. Quantitation of HIV-1-specific cytotoxic T lymphocytes and plasma load of viral RNA. Science **279**:2103–2106.
6. **Schmitz JE, Kuroda MJ, Santra S, Sasseville VG, Simon MA, Lifton MA, Racz P, Tenner-Racz K, Dalesandro M, Scallon BJ, Ghrayeb J, Forman MA, Montefiori DC, Rieber EP, Letvin NL, Reimann KA.** 1999. Control of viremia in simian immunodeficiency virus infection by $CD8^+$ lymphocytes. Science **283**:857–860.
7. **Gandhi RT, Walker BD.** 2002. Immunologic control of HIV-1. Annu. Rev. Med. **53**:149–172.
8. **Goulder PJ, Watkins DI.** 2008. Impact of MHC class I diversity on immune control of immunodeficiency virus replication. Nat. Rev. Immunol. **8**:619–630.
9. **Borrow P, Lewicki H, Wei X, Horwitz MS, Peffer N, Meyers H, Nelson JA, Gairin JE, Hahn BH, Oldstone MB, Shaw GM.** 1997. Antiviral pressure exerted by HIV-1-specific cytotoxic T lymphocytes (CTLs) during primary infection demonstrated by rapid selection of CTL escape virus. Nat. Med. **3**:205–211.
10. **Goulder PJ, Phillips RE, Colbert RA, McAdam S, Ogg G, Nowak MA, Giangrande P, Luzzi G, Morgan B, Edwards A, McMichael AJ, Rowland-Jones S.** 1997. Late escape from an immunodominant cytotoxic T-lymphocyte response associated with progression to AIDS. Nat. Med. **3**:212–217.
11. **Goulder PJ, Brander C, Tang Y, Tremblay C, Colbert RA, Addo MM, Rosenberg ES, Nguyen T, Allen R, Trocha A, Altfeld M, He S, Bunce M, Funkhouser R, Pelton SI, Burchett SK, McIntosh K, Korber BT, Walker BD.** 2001. Evolution and transmission of stable CTL escape mutations in HIV infection. Nature **412**:334–338.
12. **Moore CB, John M, James IR, Christiansen FT, Witt CS, Mallal SA.** 2002. Evidence of HIV-1 adaptation to HLA-restricted immune responses at a population level. Science **296**:1439–1443.
13. **Draenert R, Le Gall S, Pfafferott KJ, Leslie AJ, Chetty P, Brander C, Holmes EC, Chang SC, Feeney ME, Addo MM, Ruiz L, Ramduth D, Jeena P, Altfeld M, Thomas S, Tang Y, Verrill CL, Dixon C, Prado JG, Kiepiela P, Martinez-Picado J, Walker BD, Goulder PJ.** 2004. Immune selection for altered antigen processing leads to cytotoxic T lymphocyte escape in chronic HIV-1 infection. J. Exp. Med. **199**:905–915.
14. **Leslie A, Kavanagh D, Honeyborne I, Pfafferott K, Edwards C, Pillay T, Hilton L, Thobakgale C, Ramduth D, Draenert R, Le Gall S, Luzzi G, Edwards A, Brander C, Sewell AK, Moore S, Mullins J, Moore C, Mallal S, Bhardwaj N, Yusim K, Phillips R, Klenerman P, Korber B, Kiepiela P, Walker B, Goulder P.** 2005. Transmission and accumulation of CTL escape variants drive negative associations between HIV polymorphisms and HLA. J. Exp. Med. **201**:891–902.
15. **Kawashima Y, Pfafferott K, Frater J, Matthews P, Payne R, Addo M, Gatanaga H, Fujiwara M, Hachiya A, Koizumi H, Kuse N, Oka S, Duda A, Prendergast A, Crawford H, Leslie A, Brumme Z, Brumme C, Allen T, Brander C, Kaslow R, Tang J, Hunter E, Allen S, Mulenga J, Branch S, Roach T, John M, Mallal S, Ogwu A, Shapiro R, Prado JG, Fidler S, Weber J, Pybus OG, Klenerman P, Ndung'u T, Phillips R, Heckerman D, Harrigan PR, Walker BD, Takiguchi M, Goulder P.** 2009. Adaptation of HIV-1 to human leukocyte antigen class I. Nature **458**:641–645.
16. **Avila-Rios S, Ormsby CE, Carlson JM, Valenzuela-Ponce H, Blanco-Heredia J, Garrido-Rodriguez D, Garcia-Morales C, Heckerman D, Brumme ZL, Mallal S, John M, Espinosa E, Reyes-Teran G.** 2009. Unique features of HLA-mediated HIV evolution in a Mexican cohort: a comparative study. Retrovirology **6**:72. doi:10.1186/1742-4690-6-72.
17. **Boutwell CL, Essex M.** 2007. Identification of HLA class I-associated amino acid polymorphisms in the HIV-1C proteome. AIDS Res. Hum. Retroviruses **23**:165–174.
18. **Brumme ZL, Brumme CJ, Heckerman D, Korber BT, Daniels M, Carlson J, Kadie C, Bhattacharya T, Chui C, Szinger J, Mo T, Hogg RS, Montaner JS, Frahm N, Brander C, Walker BD, Harrigan PR.** 2007. Evidence of differential HLA class I-mediated viral evolution in functional and accessory/regulatory genes of HIV-1. PLoS Pathog. **3**:e94. doi:10.1371/journal.ppat.0030094.
19. **Carlson JM, Listgarten J, Pfeifer N, Tan V, Kadie C, Walker BD, Ndung'u T, Shapiro R, Frater J, Brumme ZL, Goulder PJ, Heckerman D.** 2012. Widespread impact of HLA restriction on immune control and escape pathways of HIV-1. J. Virol. **86**:5230–5243.
20. **Carlson JM, Brumme ZL, Rousseau CM, Brumme CJ, Matthews P, Kadie C, Mullins JI, Walker BD, Harrigan PR, Goulder PJ, Heckerman D.** 2008. Phylogenetic dependency networks: inferring patterns of CTL escape and codon covariation in HIV-1 Gag. PLoS Comput. Biol. **4**:e1000225. doi:10.1371/journal.pcbi.1000225.
21. **Rousseau CM, Daniels MG, Carlson JM, Kadie C, Crawford H, Pren-**

dergast A, Matthews P, Payne R, Rolland M, Raugi DN, Maust BS, Learn GH, Nickle DC, Coovadia H, Ndung'u T, Frahm N, Brander C, Walker BD, Goulder PJ, Bhattacharya T, Heckerman DE, Korber BT, Mullins JI. 2008. HLA class I-driven evolution of human immunodeficiency virus type 1 subtype C proteome: immune escape and viral load. J. Virol. 82:6434–6446.

22. Crawford H, Lumm W, Leslie A, Schaefer M, Boeras D, Prado JG, Tang J, Farmer P, Ndung'u T, Lakhi S, Gilmour J, Goepfert P, Walker BD, Kaslow R, Mulenga J, Allen S, Goulder PJ, Hunter E. 2009. Evolution of HLA-B*5703 HIV-1 escape mutations in HLA-B*5703-positive individuals and their transmission recipients. J. Exp. Med. 206:909–921.
23. Honeyborne I, Prendergast A, Pereyra F, Leslie A, Crawford H, Payne R, Reddy S, Bishop K, Moodley E, Nair K, van der Stok M, McCarthy N, Rousseau CM, Addo M, Mullins JI, Brander C, Kiepiela P, Walker BD, Goulder PJ. 2007. Control of human immunodeficiency virus type 1 is associated with HLA-B*13 and targeting of multiple gag-specific $CD8^+$ T-cell epitopes. J. Virol. 81:3667–3672.
24. Naruto T, Murakoshi H, Chikata T, Koyanagi M, Kawashima Y, Gatanaga H, Oka S, Takiguchi M. 2011. Selection of HLA-B57-associated Gag A146P mutant by HLA-B*48:01-restricted Gag140-147-specific CTLs in chronically HIV-1-infected Japanese. Microbes Infect. 13:766–770.
25. Goulder PJ, Bunce M, Krausa P, McIntyre K, Crowley S, Morgan B, Edwards A, Giangrande P, Phillips RE, McMichael AJ. 1996. Novel, cross-restricted, conserved, and immunodominant cytotoxic T lymphocyte epitopes in slow progressors in HIV type 1 infection. AIDS Res. Hum. Retroviruses 12:1691–1698.
26. Leslie AJ, Pfafferott KJ, Chetty P, Draenert R, Addo MM, Feeney M, Tang Y, Holmes EC, Allen T, Prado JG, Altfeld M, Brander C, Dixon C, Ramduth D, Jeena P, Thomas SA, St John A, Roach TA, Kupfer B, Luzzi G, Edwards A, Taylor G, Lyall H, Tudor-Williams G, Novelli V, Martinez-Picado J, Kiepiela P, Walker BD, Goulder PJ. 2004. HIV evolution: CTL escape mutation and reversion after transmission. Nat. Med. 10:282–289.
27. Miura T, Brockman MA, Schneidewind A, Lobritz M, Pereyra F, Rathod A, Block BL, Brumme ZL, Brumme CJ, Baker B, Rothchild AC, Li B, Trocha A, Cutrell E, Frahm N, Brander C, Toth I, Arts EJ, Allen TM, Walker BD. 2009. HLA-B57/B*5801 human immunodeficiency virus type 1 elite controllers select for rare gag variants associated with reduced viral replication capacity and strong cytotoxic T-lymphocyte recognition. J. Virol. 83:2743–2755.
28. Kawashima Y, Kuse N, Gatanaga H, Naruto T, Fujiwara M, Dohki S, Akahoshi T, Maenaka K, Goulder P, Oka S, Takiguchi M. 2010. Long-term control of HIV-1 in hemophiliacs carrying slow-progressing allele HLA-B*5101. J. Virol. 84:7151–7160.
29. Akari H, Arold S, Fukumori T, Okazaki T, Strebel K, Adachi A. 2000. Nef-induced major histocompatibility complex class I down-regulation is functionally dissociated from its virion incorporation, enhancement of viral infectivity, and CD4 down-regulation. J. Virol. 74:2907–2912.
30. Falk K, Rotzschke O, Takiguchi M, Gnau V, Stevanovic S, Jung G, Rammensee HG. 1995. Peptide motifs of HLA-B51, -B52 and -B78 molecules, and implications for Behcet's disease. Int. Immunol. 7:223–228.
31. Tomiyama H, Fujiwara M, Oka S, Takiguchi M. 2005. Cutting edge: epitope-dependent effect of Nef-mediated HLA class I down-regulation on ability of HIV-1-specific CTLs to suppress HIV-1 replication. J. Immunol. 174:36–40.
32. Tomiyama H, Akari H, Adachi A, Takiguchi M. 2002. Different effects of Nef-mediated HLA class I down-regulation on human immunodeficiency virus type 1-specific CD8(+) T-cell cytolytic activity and cytokine production. J. Virol. 76:7535–7543.
33. Takamiya Y, Schonbach C, Nokihara K, Yamaguchi M, Ferrone S, Kano K, Egawa K, Takiguchi M. 1994. HLA-B*3501-peptide interactions: role of anchor residues of peptides in their binding to HLA-B*3501 molecules. Int. Immunol. 6:255–261.
34. Huang KH, Goedhals D, Carlson JM, Brockman MA, Mishra S, Brumme ZL, Hickling S, Tang CS, Miura T, Seebregts C, Heckerman D, Ndung'u T, Walker B, Klenerman P, Steyn D, Goulder P, Phillips R, Bloemfontein-Oxford Collaborative Group, van Vuuren C, Frater J. 2011. Progression to AIDS in South Africa is associated with both reverting and compensatory viral mutations. PLoS One 6:e19018. doi:10.1371/journal.pone.0019018.
35. Altman JD, Moss PA, Goulder PJ, Barouch DH, McHeyzer-Williams MG, Bell JI, McMichael AJ, Davis MM. 1996. Phenotypic analysis of antigen-specific T lymphocytes. Science 274:94–96.
36. Kabsch W. 2010. XDS. Acta Crystallogr. D Biol. Crystallogr. 66(Pt 2):125–132.
37. Evans PR. 1993. Proceedings of the CCP4 Study Weekend on Data Collection & Processing. Daresbury Laboratory, Warrington, United Kingdom.
38. Matthews BW. 1968. Solvent content of protein crystals. J. Mol. Biol. 33:491–497.
39. Vagin A, Teplyakov A. 1997. MOLREP: an automated program for molecular replacement. J. Appl. Crystallogr. 30:1022–1025.
40. Murshudov GN, Vagin AA, Dodson EJ. 1997. Refinement of macromolecular structures by the maximum-likelihood method. Acta Crystallogr. D Biol. Crystallogr. 53:240–255.
41. Adams PD, Afonine PV, Bunkoczi G, Chen VB, Davis IW, Echols N, Headd JJ, Hung LW, Kapral GJ, Grosse-Kunstleve RW, McCoy AJ, Moriarty NW, Oeffner R, Read RJ, Richardson DC, Richardson JS, Terwilliger TC, Zwart PH. 2010. PHENIX: a comprehensive Python-based system for macromolecular structure solution. Acta Crystallogr. D Biol. Crystallogr. 66:213–221.
42. Laskowski RA, MacArthur MW, Moss DS, Thornton JM. 1993. PROCHECK: a program to check the stereochemical quality of protein structures. J. Appl. Crystallogr. 26:283–291.
43. Emsley P, Lohkamp B, Scott WG, Cowtan K. 2010. Features and development of Coot. Acta Crystallogr. D Biol. Crystallogr. 66:486–501.
44. Sakaguchi T, Ibe M, Miwa K, Yokota S, Tanaka K, Schonbach C, Takiguchi M. 1997. Predominant role of N-terminal residue of nonamer peptides in their binding to HLA-B* 5101 molecules. Immunogenetics 46:245–248.
45. Maenaka K, Maenaka T, Tomiyama H, Takiguchi M, Stuart DI, Jones EY. 2000. Nonstandard peptide binding revealed by crystal structures of HLA-B*5101 complexed with HIV immunodominant epitopes. J. Immunol. 165:3260–3267.
46. Sakaguchi T, Ibe M, Miwa K, Kaneko Y, Yokota S, Tanaka K, Takiguchi M. 1997. Binding of 8-mer to 11-mer peptides carrying the anchor residues to slow assembling HLA class I molecules (HLA-B*5101). Immunogenetics 45:259–265.
47. Hiraiwa M, Yamamoto J, Matsumoto K, Karaki S, Nagao T, Kano K, Takiguchi M. 1991. T cell can recognize the allospecificities formed by the substitution of amino acids associated with HLA-Bw4/Bw6 public epitopes. Hum. Immunol. 32:41–45.
48. Yamamoto J, Hiraiwa M, Hayashi H, Tanabe M, Kano K, Takiguchi M. 1991. Two amino acid substitutions at residues 63 and 67 between HLA-B51 and HLA-Bw52 form multiple epitopes recognized by allogeneic T cells. Immunogenetics 33:286–289.
49. Tomiyama H, Sakaguchi T, Miwa K, Oka S, Iwamoto A, Kaneko Y, Takiguchi M. 1999. Identification of multiple HIV-1 CTL epitopes presented by HLA-B*5101 molecules. Hum. Immunol. 60:177–186.
50. Zhang Y, Peng Y, Yan H, Xu K, Saito M, Wu H, Chen X, Ranasinghe S, Kuse N, Powell T, Zhao Y, Li W, Zhang X, Feng X, Li N, Leligdowicz A, Xu X, John M, Takiguchi M, McMichael A, Rowland-Jones S, Dong T. 2011. Multilayered defense in HLA-B51-associated HIV control. J. Immunol. 187:684–691.

厚生労働科学研究費補助金エイズ対策研究事業
「多施設共同研究を通じた新規治療戦略作成に関する研究」班
平成22-24年度　総合研究報告書

発行日　2013年3月29日

発行者　研究代表者　岡　慎一

発行所　研究班事務局
(独)国立国際医療研究センター
エイズ治療・研究開発センター
〒162-8655　東京都新宿区戸山1-21-1